Development of Sclerosing Cholangitis in Mdr2 (Abcb4) Knockout Mice- A Longitudinal Study in Aging Mice

eingereicht von

Florian Reiter

Mat.Nr.: 0433321

zur Erlangung des akademischen Grades

Doktor der gesamten Heilkunde

(Dr. med. univ.)

an der

Medizinischen Universität Graz

ausgeführt an der

Medizinischen Universitätsklinik

Abteilung für Gastroenterolgie und Hepatologie

unter der Anleitung von

Prof. Dr. Michael Trauner und Doz. Dr. Peter Fickert

Ort, Datum …….. (Unterschrift)

Eidesstattliche Erklärung

Ich erkläre ehrenwörtlich, dass ich die vorliegende Arbeit selbstständig und ohne fremde Hilfe verfasst habe, andere als die angegebenen Quellen nicht verwendet habe und die den benutzten Quellen wörtlich oder inhaltlich entnommenen Stellen als solche kenntlich gemacht habe.

Graz, am …… *Unterschrift*

Danksagung

Herrn Univ. Prof. Dr. Michael Trauner und Univ. Doz. Dr. Peter Fickert möchte ich für ihr Bemühen und ihre Betreuung bei der Erstellung dieser Arbeit danken.

Mein ganz besonderer Dank geht an Sabine Halsegger, Dagmar Silbert und Judith Gumhold sowie allen Mitarbeitern des Labors für molekulare und experimentelle Hepatologie Graz, die mich sowohl in technischer als auch persönlicher Hinsicht sehr unterstützt haben.

Ganz besonders danke ich meinen Eltern, die mir das Studium der Medizin ermöglicht haben und in mir das Interesse für die Wissenschaft geweckt haben.

Weiters möchte ich meinen Großeltern danken, welchen ich diese Arbeit, für ihre herzliche und liebevolle Unterstützung, widmen möchte.

Schließlich bedanke ich mich auch für das Korrekturlesen meiner Arbeit durch Dr. Thierry Claudel und Franz Ferk.

Dedicated to my grandparents

Meinen Großeltern gewidmet

Abstract

Deutsch

Hintergrund und Ziele: Die Primär Sklerosierende Cholangitis (PSC) stellt ein chronisch cholestatische Lebererkrankung dar, die oft eine Leberzirrhose verursacht und eine Lebertransplantation notwendig macht. Trotz intensiver Forschung ist die Pathogenese dieser Erkrankung noch wenig verstanden. Durch das Ausschalten des Mdr2 Gens entsteht ein Mausmodell, welches histologische Charakteristika der PSC, wie die zwiebelschalenartige Fibrose als auch porto-portale Fibrose, aufweist. Mdr2 Knockout Mäuse weisen nach kurzer Zeit eine ausgeprägte Entzündung und Fibrose der Leber auf, die im weiteren Verlauf auch zu einem hepatozellulären Karzinom führen kann. Bis *dato* gibt es nur wenige Daten bezüglich der zeitlichen Entwicklung von Entzündung und Fibrose im Alterungsprozess dieser Mäuse sowie möglicher geschlechtsspezifische Unterschiede. Ein wichtiger Punkt wäre es auch zu klären, ob die Mäuse in einem späten Krankheitsstadium eine Zirrhose entwickeln, welche in Mausmodellen bislang noch nicht beobachtet werden konnte.

Material und Methoden: Leberproben von Knockoutmäusen wurden retrospektiv in sechs Gruppen im Lebensalter von 6 bis 13 Monaten eingeteilt: 6 bis 7 Monate; 9 bis 10 Monate; 11 bis 13 Monate. Die zeitliche Entwicklung und Geschlechtsunterschiede von relevanten Parametern für Leberfunktion, histologischem Phänotyp, Fibrose, Entzündung sowie duktularer Proliferation wurden mittels Serumbiochemie, H&E und Sirius-red Färbung, Real-time PCR, Immunhistochemie und Western Blot untersucht.

Resultate: Mdr2 Knockout Mäuse zeigten bis zu einem Alter von 13 Monaten keine Entwicklung einer biliären Zirrhose, während typische histologische Zeichen cholestatischer Leberschädigung gefunden wurden. Sowohl signifikant unterschiedliche Mengen an Hydroxyprolin beziehungsweise Unterschiede in der CK19 mRNA Expression zwischen den männlichen und weiblichen Tieren (6 bis 7 Monate alte Gruppen), als auch eine ungleiche F4/80 und IL-1β Expression zwischen den 9 bis 10 Monate alten Tieren, konnten in dieser Studie gefunden werden. Es

wurden keine geschlechtsbezogenen sowie altersbezogenen signifikanten Unterschiede hinsichtlich der Entwicklung der Leberfunktion, der Expression relevanter Gene und Proteine für Fibrose, duktulare Proliferation als auch Entzündung sowie der hepatozellulären Proliferation gefunden.

Schlussfolgerungen: Die hepatische Entzündung und Fibrose zeigte im frühen Krankheitsverlauf eine stärkere Ausprägung in den weiblichen Tieren, jedoch glichen sich die männlichen Tiere zu einem späteren Zeitpunkt an. Weder in den männlichen noch den weiblichen Tieren konnte eine deutliche Progression der Lebererkrankung bis hin zur Leberzirrhose gefunden werden. Weiterführende Studien sollten die Mechanismen die zur Stabilisierung des Kranksheitsbildes beitragen identifizieren, um mögliche therapeutische Interventionen davon ableiten zu können.

English

Background and Aims: Primary sclerosing cholangitis (PSC) represents a chronic cholestatic liver disease frequently leading to liver cirrhosis and the need for liver-transplantation. Despite intensive research on the pathogenesis of PSC it is still widely unknown. Disruption of the Mdr2 (Abcb4) gene results in a mouse model which displays histological features of human PSC such as onion skin like periductal fibrosis and liver fibrosis of the biliary type. After delivery and starting suckling Mdr2 (-/-) mice develop severe inflammation and fibrosis of the liver, which can lead to a hepatocellular carcinoma in elder mice. To date little is known on the time course of inflammation and fibrosis as well as gender specific differences. Furthermore it is important to clarify if Mdr2 (-/-) mice develop liver cirrhosis, which can often be seen in patients suffering from PSC but could yet not be observed in rodent models.

Material and Methods: Frozen liver tissue of Mdr2 (-/-) mice (obtained from the Jackson Laboratory, Bar Harbor, MA) was arranged retrospectively in six groups out of a period ranging from 6 to 13 months: 6 to 7 months; 9 to 10 months; 11 to 13 months. Development and potential gender differences in liver function, histological phenotype, fibrosis, inflammation as well as ductular proliferation were examined by analyzing serum biochemistry, H&E staining, Sirius red staining, real-time PCR, immuno-histochemistry and Western blot.

Results: Mdr2 (-/-) mice did not develop biliary cirrhosis, while the characteristic histological pattern of cholestatic liver disease was found. Significant differences in hydroxyproline content, CK19 mRNA expression between male and female animals (6-7 month old groups), as well as differences in F4/80 and IL-1β mRNA expression levels between 9 to 10 month-old groups, were detected in this study. We found no gender or age specific differences in regard to liver function, expression of genes and proteins relevant for inflammation, fibrosis, ductular and hepatocellular proliferation were observed.

Conclusion: In young mice hepatic inflammation and fibrosis were more pronounced in female mice. However the extent of liver damage in males aligned itself a later

point. Neither male nor female mice showed progression to liver cirrhosis. Future studies should determine potential factors leading to stabilization of the cholestatic phenotype in Mdr2 (-/-) mice since such mechanisms could unravel potential future therapeutic targets.

Table of contents

Deutsch 5
English 7
List of Figures and Tables 11
List of Abbreviations 12
1 Introduction 14
1.1 Liver Physiology 14
1.1.1 Physiology of Bile Formation and Hepatobiliary Transport Systems 14
1.1.2 The Canalicular Mdr2/MDR3 Efflux Pump 16
1.2 Bile 17
1.2.1 Bile Acids: Synthesis, Metabolism and Function 17
1.2.2 Phospholipids and Cholesterol in Bile 19
1.2.3 The Toxic Bile Concept 20
1.3 Cholestasis 21
1.3.1 Definition 21
1.3.2 The MDR3 Transporter in Human Liver Disease 21
1.3.3 Primary Sclerosing Cholangitis 22
1.4 Mdr2 (-/-) Mouse Model of Sclerosing Cholangitis and Biliary Fibrosis 24
1.4.1 Sclerosing Cholangitis 24
1.4.2 Carcinogenesis in Mdr2 (-/-) Mice 24
1.4.3 Gender Differences in Mdr2 (-/-) Mice 26
2 Aims of the Study 27
3 Materials and Methods 28
3.1 Animals 28
3.2 Hematoxylin and Eosin Staining (H&E Stain) 28
3.3 Sirius Red Staining 30
3.4 Immunohistochemistry 32
3.5 Serum Biochemistry 35
3.6 Determination of Hepatic Hydroxyproline Content 35
3.7 Messenger RNA Analysis and Polymerase Chain Reaction (PCR) 37

3.7.1 RNA Isolation 37
3.7.2 RNA Photometry 38
3.7.3 RNA Electrophoresis 38
3.7.4 Transcription of RNA into cDNA 39
3.7.5 Sybr® Green Real-Time Polymerase Chain Reaction (PCR) 41
3.8 Western Blot 42
3.8.1 Tissue Preparation 43
3.8.2 Gel-electrophoresis 44
3.8.3 Transfer (Electroblotting) 46
3.8.4 Blocking of Membrane 47
3.8.5 Immunoreaction and Detection 48
3.9 Statistical Analysis 49
4 Results 50
4.1 Serum Biochemistry and Cell Proliferation 50
4.1.1 Serum Biochemistry 50
4.1.2 Cellular Proliferation Reflected by Ki-67 Positive Cells 51
4.2 Fibrosis 52
4.2.1 Sirius Red Staining 52
4.2.2 Hydroxyproline Content 54
4.2.3 α-Sma Immunohistochemistry 55
4.2.4 Fibrosis Gene Expression 57
4.2.5 Do Mdr2 (-/-) Mice Develop Liver Cirrhosis? 58
4.3 Inflammation 59
4.4 Ductular Proliferation 60
5 Discussion 62
6 References 67

List of Figures and Tables

Figure 1: Hepatocellular transporters of normal hepatocytes. 15
Figure 2: Toxic bile concept. 20
Figure 3: Course of liver disease in Mdr 2 (-/-) mice. 25
Figure 4: H&E staining of a normal mouse liver 29
Figure 5: Sirius red staining of a normal mouse liver 31
Figure 6: RNA electrophoresis-gel. 39
Figure 7: Results serum biochemistry 50
Figure 8: Results counting Ki-67 positive hepatocytes 51
Figure 9: Periportal fibrosis (sirius red) 52
Figure 10: Lobular fibrosis (sirius red). 53
Figure 11: Hydroxyproline measurement 54
Figure 12: αSma immunohistochemistry 55
Figure 13: Western blot analysis of αSma protein 56
Figure 14: mRNA expression of fibrosis relevant genes 57
Figure 15: H&E sections of 13 month-old knockout mouse 58
Figure 16: mRNA expression of inflammation relevant genes 59
Figure 17: CK19 immunohistochemistry 60
Figure 18: Western blot analysis of CK19 protein 61
Figure 19: CK19 mRNA expression 61

Table 1: Antibodies used for immunohistochemistry 32
Table 2: Antigen and their specificity 32
Table 3: Antibodies used for Western blotting 42

List of Abbreviations

α-Sma	**α-Smooth muscle actin**
Abc	**ATP-binding cassette**
ABCB 4	**ATP-binding cassette subfamily B member 4**
ABCG 5/8	**ATP-binding cassette subfamily G member 5/8**
ALT	**Alanine transaminase**
ALP	**Alkaline phospatase**
ANCA	**Anti-neutrophil-cytoplasmatic-antibodies**
AST	**Aspartate transaminase**
ATP	**Adenosine triphosphate**
BA	**Bile acids**
Bili	**Bilirubin**
BSEP	**Bile salt export pump**
CCC	**Cholangiocellular carcinoma**
cDNA	**Complementary deoxyribonucleic acid**
Cftr	**Cystic fibrosis transmembrane conductance regulator**
Chol	**Cholesterol**
CK19	**Cytokeratin 19**
Col1a1	**Collagen type 1 alpha 1**
CYP7a1	**Cholesterol-7α hydroxylase**
CYP27a1	**Sterol-27-alpha hydroxylase**
DNA	**Deoxyribonucleic acid**
ERCP	**Endoscopic-retrograde-cholangiopancreatography**
Fc	**Fragment crystallizable region/portion**
FXR	**Farnesoid X receptor**
HDL	**High density lipoprotein**
HLA	**Human leukocyte antigen**
H&E	**Hematoxylin and eosin staining**
HRP	**Horseradish peroxidase**
IBD	**Inflammatory bowel disease**
Il-1β	**Interleukin 1β**
LDL	**Low density lipoprotein**

LPAC	**Low-phospholipid-associated cholelithiasis syndrome**
MCP-1	**Monocyte chemotactic protein-1**
Mdr2	**Multidrug-resistance-2 P glycoprotein**
MDR3	**Multidrug-resistance protein 3**
Mmp13	**Matrix metalloproteinase 13**
MRCP	**Magnetic resonance cholangiopancreatography**
MRP3	**Multidrug-resistance associated protein 3**
MRP4	**Multidrug-resistance associated protein 4**
N	**Number**
NF-kB	**Nuclear factor kB**
NTCP	**Sodium taurocholate co-transporting polypeptide**
OATP	**Organic-anion transporter**
OSTα/β	**Organic solute transporter α/β**
PBC	**Primary biliary cirrhosis**
PCR	**Polymerase chain reaction**
PFIC 3	**Progressive familial intrahepatic cholestasis type 3**
PL	**Phospholipids**
PSC	**Primary sclerosing cholangitis**
RNA	**Ribonucleic acid**
Timp	**Tissue inhibitor of metalloproteinases 1**
TNF-α	**Tumour necrosis factor α**
UDCA	**Ursodeoxycholic-acid**
VLDL	**Very low density lipoprotein**

1 Introduction

1.1 Liver Physiology

1.1.1 Physiology of Bile Formation and Hepatobiliary Transport Systems

The human liver is responsible for a wide range of vital functions. In addition to biosynthesis as well as breakdown of vitally important proteins (e.g acute phase proteins, coagulation factors), the liver also plays a key role in metabolism (e.g. glycogenolysis, glycogenesis, glyconeogenesis, lipid metabolism, cholesterol synthesis) [1] .

The liver functions as a major excretion organ and enables the elimination of waste substances via bile. The physiologic transport processes in the hepatobiliary system, are provided by hepatocellular transporters necessary for the uptake and secretion of molecules along the hepatic canaliculi (Figure 1). Uptake of bile salts and other molecules take place on the basolateral membrane or sinusoidal surface of the hepatocytes (Figure 1). In contrast, the secretory transport systems are located on the canalicular plasma membrane (Figure 1). Furthermore the secretion of bile also depends on the adsorptive and secretory transporters of biliary epithelial cells. The sodium-taurocholate-cotransporting-peptide (NTCP) is necessary for translocating conjugated bile salts from the portal blood into the cytoplasm. A sodium independent translocation of unconjugated bile salts and other lipophilic albumin-bound molecules is provided by the organic-anion transporting-peptide (OATP). On the canalicular side proteins are located which regulate the excretory functions of the hepatocytes. The bile salt export pump (BSEP) mediates the excretion of bile salts into bile. The multidrug-resistance-3 P-glycoprotein (MDR3), which is the human homologue of the multidrug-resistance-2 P glycoprotein (Mdr2/Abcb4) in rodents, is necessary to translocate phospholipids into bile in order to enable the formation of micelles in bile. ABCG5/8 are hemi transporters excreting cholesterol into the bile (Figure 1). There are also some alternative bile salt export pumps on the basolateral side of the

hepatocytes that normally are expressed at low levels, but can be up-regulated under cholastatic conditions concering the multidrug-resistance associated protein 3 (MRP3), multidrug-resistance associated protein 4 (MRP4) and the organic solute transporter α/β (OSTα/β) (Figure 1) [2,3].

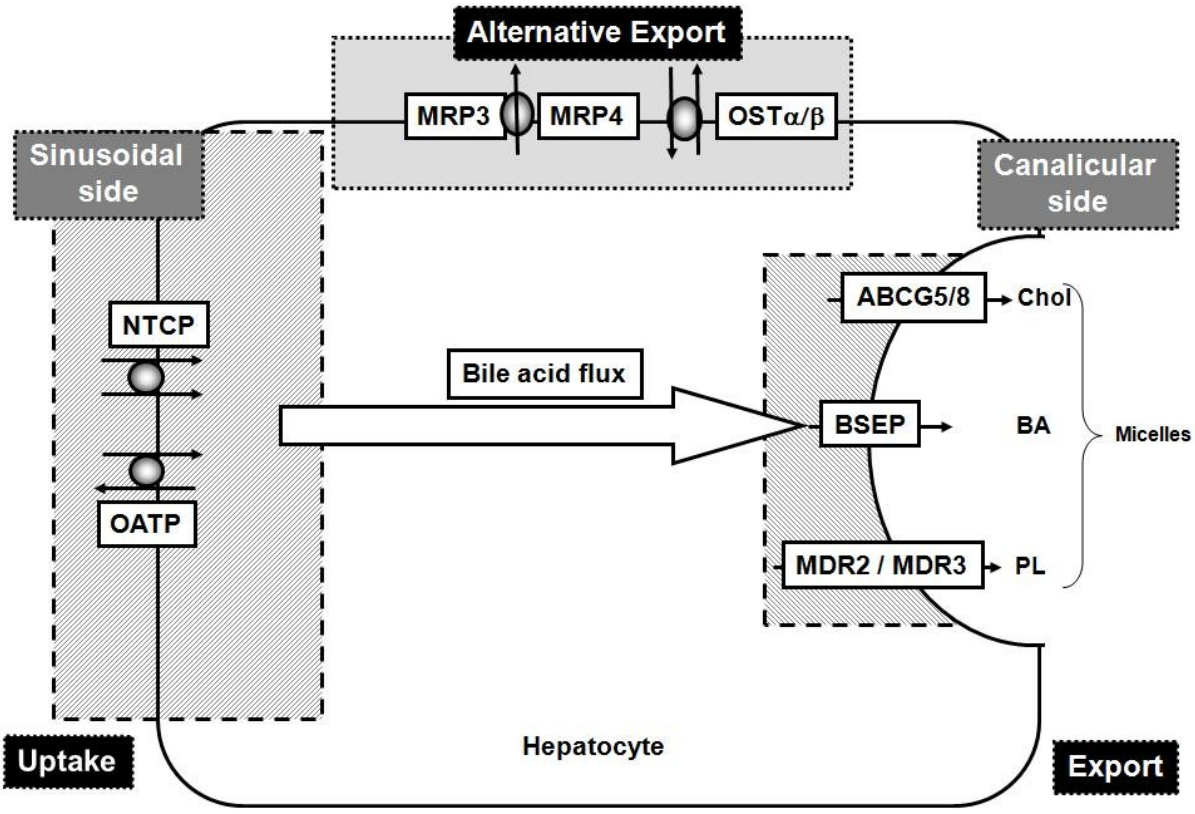

Figure 1: Hepatocellular transporters of normal hepatocytes. ATP-binding cassette subfamily G member 5/8 (ABCG5/8), Bile acids (BA), Bile salt expot pump (BSEP), Cholesterin (Chol), Multi drug resistance protein 2/3 (MDR2/3), Multidrug-resistance associated protein 3 (MRP3), Multidrug-resistance associated protein 4 (MRP4), Sodium taurocholate co-transporting polypeptide (NTCP), Organic-anion transporter (OATP), Organic solute transporter α/β (OSTα/β), Phospholipids (PL);

1.1.2 The Canalicular Mdr2/MDR3 Efflux Pump

MDR3 (ABCB4) belongs to the ATP-binding cassette transporters family (ABC). ABC transporter represent a large family of membrane proteins with diverse properties and functions. These proteins create the energy for the transport processes via hydrolysis of adenosine triphosphate (ATP). Mdr2/MDR3 transporter is a phospholipid floppase and translocates phospatidylcholine from the inner to the outer leaflet of the canalicular membrane to form mixed micelles together with bile salts and cholesterol (Figure 1) [4].

1.2 Bile

1.2.1 Bile Acids: Synthesis, Metabolism and Function

Bile acids (BAs) are the major component of bile and represent the end product of cholesterol catabolism. BA synthesis occurs in hepatocytes and is permitted by a cascade of 12 enzymatic reactions [5]. The rate limiting step represents the hydroxylation of cholesterol by the cholesterol-7α-hydroxylase (CYP7a1) which can only be found in liver. In addition, an alternative pathway called the acidic pathway exists, which occurs in numerous extrahepatic tissues and is initialized by the sterol-27-hydroxylase (CYP27a1) [5]. BAs are modified by conjugation with taurine or glycine in order to make them more hydrophilic. Thereby, BAs are no longer permeable through cell membranes and specific transporters are needed for their uptake and secretion. BAs are conserved under normal conditions. After the secretion into bile, BAs are reabsorbed in the distal ileum and re-enter the blood circulation. They are absorbed by the liver and are secreted into bile again (i.e. the enterohepatic circulation). Thereby the conjugated BAs are modified by bacterial enzymatic reactions. These reactions are causing the unconjugation as well as the loss of a hydroxyl group. This kind of modification causes the distinction between primary and secondary BAs (e.g. primary bile acid: Cholic-acid→ secondary bile acid: Deoxycholic-acid) [6].

In 1999 Hofman summarized five major physiological functions of bile which are now well established [7]. First, the excretion of cholesterol by transforming it into BAs, which enables the elimination via the faecal route. Second, the emulsifying effects of BAs on lipids in the intestine providing thereby the lipid uptake including nutrimental lipids as well as vitamins (A,D,E,K). Third, stimulation of bile flow and fourth, stimulation of phosopholipid secretion. BAs induce both bile flow via their osmotic properties and a higher excretion of phospholipids into bile, which results in a greater fraction of BAs existing in form of mixed micelles. Fifth, the amount of BAs in the hepatocytes seems to act as a signal for BA biosynthesis, since a high level of intracellular BA content lowers bile synthesis and *vice versa* [7]. Currently BAs are also recognized as important signal molecules affecting energy homeostasis as well as glucose and lipid metabolism. The natural BAs nuclear receptor Farnesoid X Receptor (FXR), is supposed to play a major role in this regard [8]. A high

transhepatic BA flux results in FXR activation and thereby lowers the cholesterol elimination and causes an elevation of low density lipoprotein (LDL) cholesterol as well as a decrease of the high density lipoprotein (HDL) bound cholesterol [8]. Furthermore it is well known that a high BA level reduces the production of very low density lipoprotein (VLDL) and thereby lower the severity of hypertriglyceridaemia [8]. In terms of energy homeostasis BAs also affect the development of diet-induced obesity and hyperglygaemia in rodents [8]. It is known that the administration of BAs leads to a higher energy expenditure in brown adipose tissue with preventive effects on obesity and hyperglycaemia. However these effects are supposed to be FXR-independent, but are mediated via the activation of a G-protein-coupled BA receptor, also known as TGR5, which represents a membrane BA receptor [8]. In addition BA increase glycogenesis, inhibit gluconeogenisis and in this manner improve hyperglycaemia [8]. Recently there is new evidence of FXR activation and its role in hepatic inflammation [9]. These effects were confirmed in the FXR knockout mouse model. These knockout mice are developing a pronounced inflammation, with a high expression of inflammatory genes in the liver [9]. Furthermore the mice are developing massive necrosis after lipopolysaccharide administration in contrast to the control group of wild type animals [9]. In addition the activation of FXR in animal models for non-alcoholic fatty liver disease suggests an inhibition of inflammation and fibrosis [9]. Currently it is known that an insufficient BA accumulation in the intestine is leading to a bacterial overgrowth. This overgrowth can be reversed with the oral administration of BAs, however the extent of this effect is not totally explainable with the antibacterial properties of BAs [9]. The findings of bacterial overgrowth and large amounts of bacteria in the mesenteric lymph nodes in FXR knockout mice implicate the BA-FXR pathway as relevant for intestinal barrier function and bacterial defence [9].

1.2.2 Phospholipids and Cholesterol in Bile

BAs, phospolipids and cholesterol reflect the major constitutents of bile [8]. The export of these lipids into bile is provided by transporters mentioned in chapter 1.1.1 (Figure 1). It is known that the biliary lipid excretion is driven by BAs [10]. The excretion of cholesterol from the body is essential and eliminated via the faecal route either directly or after the conversion into BAs. Thereby it reflects the most important elimination pathway of cholesterol. A large part of these lipids is reabsorbed in the intestine [10]. Furthermore the secretion of phospholipids into bile enables the solubilisation of cholesterol and thereby prevents the formation of gallstones. The Mdr2/MDR3 represents the canalicular floppase, which mediates the transport of phospholipids into bile [11,12]. While the transport of cholesterol into bile is provided by the hemi transporters ABCG5/8 [3].Since bile is already under normal conditions toxic [13], an accurate excretion of phospholipids as well as cholesterol is needed in order to build micelles together with BAs. Beside this accurate formation of bile in regard of micellar binding of bile acids, bile hydration, alkalinisation, mucin formation as well as bile flow are necessary for preventing bile duct injury via the detergent properties of BA [3].

1.2.3 The Toxic Bile Concept

The accurate formation of bile is a vital function and enables not only the solution and absorption of nutritional lipids but also the protection of the bile duct from the detergent properties of BAs. Under normal conditions BAs form mixed micelles together with phospholipids and cholesterol in order to create a hydrophilic surface. Alterations in the composition of bile with an enhancement of hydrophobic BAs are leading to toxic bile, with higher detergent properties. Thereby the BAs are eluting lipids like phospolipids and cholesterol from cell membranes [11]. This hypothesis explains, why the liver damge in Mdr2 (-/-) mice occures not until 2 days of age, since the bile flow increases after birth [11]. The lack of phospholipids in Mdr 2 (-/-) mice could therefore result in toxic BA induced bile duct damage. These mice spontaneously develop bile duct injury closely resembling the liver phenotype in human SC [12]. Other factors which are causing damage of the bile duct system by increasing the toxic bile properties, in fact under bile stasis, are biliary casts and elevated biliary pressure [13].

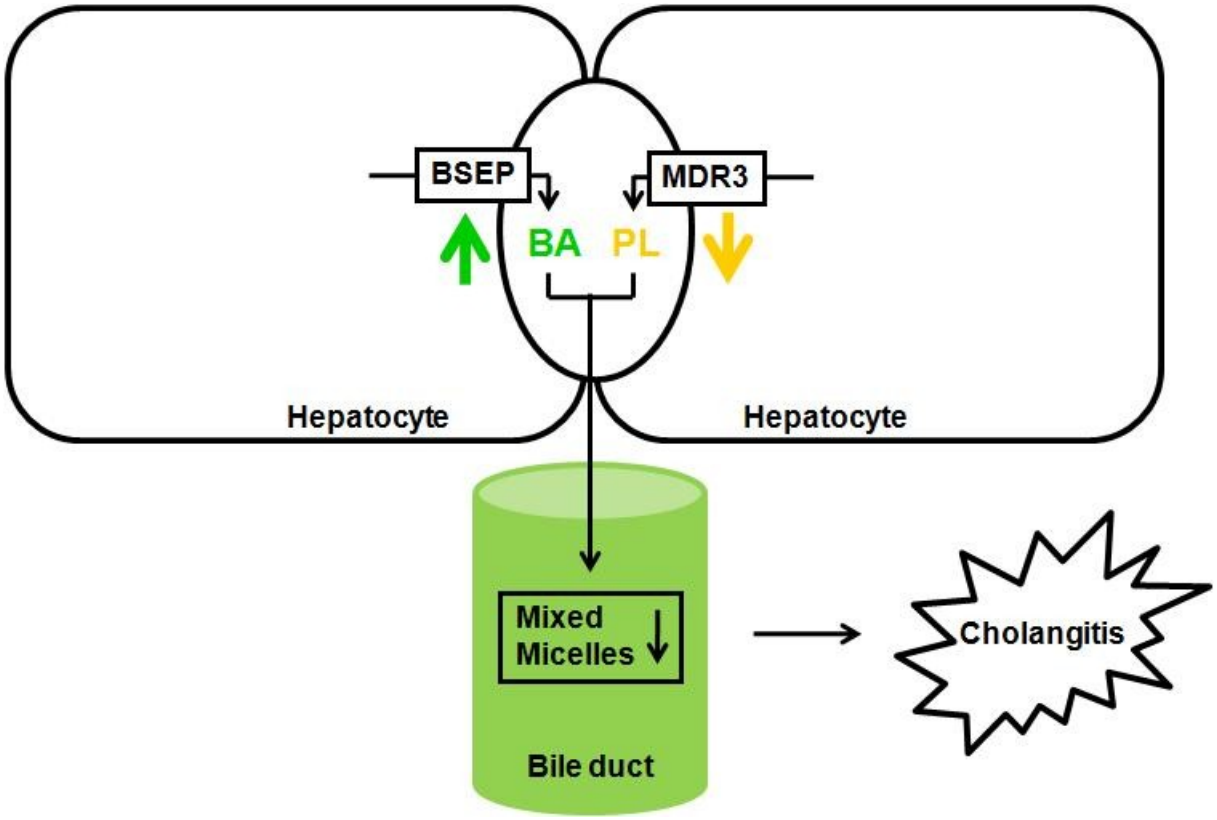

Figure 2: The figure shows the transporter alterations which are supposed to cause a "toxic bile". A low excretion of phospholipids (PL) results in a bile acid (BA)-rich bile content and leads to cholangitis.

1.3 Cholestasis

1.3.1 Definition

Cholestasis represents a condition of impaired bile flow (i.e. less bile reaches the duodenum). This can either be the result of impaired bile secretion or obstructive processes in the bile duct system. Functional defects at the level of hepatocytes are caused by a wide spectrum of genetic transporter defects (e.g. progressive familial intrahepatic cholestasis PFIC), exposure to procholestatic drugs (e.g., cyclosporine) or inflammation (e.g. sepsis). In contrast, bile duct obstruction (e.g. stones, tumors), inflammatory processes or loss of bile ducts (e.g. vanishing bile duct syndromes, primary biliary cirrhosis or primary sclerosing cholangitis) are also leading to cholestasis [14].

1.3.2 The MDR3 Transporter in Human Liver Disease

Mutations of this floppase lead to a severe kind of liver disease, the progressive familial intrahepatic cholastasis type 3 (PFIC 3). PFIC 3 represents a progressive cholestatic disease that occurs already during infancy. The pathogenesis appears to be related to the defect in phospholipid secretion and the detergent properties of hydrophobic BAs that become aggravated by a lower amount of phosphatidylcholine.

Certain variants of the MDR3 gene are associated with a syndrome reffered to as low-phospholipid-associated cholelithiasis syndrome (LPAC). The disease is characterized by an increased susceptibility to intra- and extrahepatic gallstones and pregnancy-induced cholestasis.

Furthermore MDR3 mutations seem to be a predisposing factor in cholestatic liver diseases like pregnancy- or drug-induced cholangitis. The pregnancy-induced cholangitis develops under high levels of sex hormones and causes cholestasis in pregnant women who do not show cholestatic changes under normal conditions. Women who developed intra-hepatic cholestasis of pregnancy show an elevated susceptibility for gallstones and therefore may develop chronic liver disease. The

drug-induced cholangitis is observed under treatment with verapamil or cyclosporine A, which are transported via the MDR3 floppase [15], therefore interactions between MDR3 polymorphisms and drug treatment could result in impaired phospholipid excretion [16]. In addition, MDR3 alterations seem to play a role in the progression of PSC especially in combination with other transporter polymorphism as shown for OST α/β defects [17]. Polymorphisms of the MDR3 gene are assumed to affect the disease progression and the response to therapy in PBC and PSC [16, 18;19;20;].

1.3.3 Primary Sclerosing Cholangitis

PSC is a chronic cholestatic liver disease, with unknown aetiology. PSC affects the large extra- and intrahepatic bile ducts and causes obliterative fibrosis. This disorder is normally diagnosed in younger and middle-aged patients and occurs with a 2:1 male predominance [21]. This type of cholangitis is frequently (at about three quarters) associated with an inflammatory bowel disease (IBD), especially ulcerative colitis but also in Crohn`s disease patients. Besides liver failure and liver cirrhosis, the development of cholangiocarcinoma in one third of the patients suffering from PSC is a frequent the the most severe complication [21]. At the time of diagnosis, the disorder usually appears as a cholestatic alteration of liver biochemistry, with an elevation of the alkaline phospatase and appearance of nonspecific serum antibodies such as atypical anti-neutrophil-cytoplasmatic-antibodies (ANCA). Further characteristics of this disease are strictures of the large extra- and intrahepatic bile ducts that are normally detected by using endoscopic-retrograde-cholangiopancreaticography (ERCP) or magnetic resonance cholangiopancreatography (MRCP). The typical histological features which can be found in human PSC are ductopenia of the medium and large ducts, onion-skin fibrosis, septal fibrosis, bridging necrosis and finally biliary cirrhosis. Although a relative high number of the patients are asymptomatic (15-55%), symptoms like fatigue, pruritus, jaundice, abdominal pain, weight loss, fever and hyperpigmentation are commomly reported at the time of diagnosis. The etiopathogenesis of PSC is still poorly understood as the lymphocytic infiltration of the bile ducts and the common association with other autoimmune diseases, like IBD or diabetes mellitus as well as thyroid disorders, make it likely to be an immune-mediated disorder. However, there

is still no direct proov for this concept. In addtion, none of the immune-suppressive regiments tested so far was able to significantly improve the disesase course of PSC [21]. Therefore, it is unlikely that PSC is a typical autoimmune disorder. The fact that this type of cholangitis is often associated with IBD leads to the assumption that bacterial translocation from the gut could affect the liver. Besides others a major point of criticism regarding this hypothesis is that PSC can also occur years after colectomy [21]. Therefore investigators postulated that T-lymphocytes sensitized in the gut are subsequently stored in the liver for years and activated by sofar unknown factors. An alternative hypothesis favours an association between certain HLA variants and a higher susceptibility for PSC [21]. Although the Mdr2 (-/-) model imitates many pathological features of PSC, no alterations in the expression of the human analogue (MDR3) floppase were found in liver tissue from patients who are suffering from PSC [21]. However, some studies suggest that MDR3 gene mutations and polymorphisms could play a role as a modifier gene [16].

1.4 Mdr2 (-/-) Mouse Model of Sclerosing Cholangitis and Biliary Fibrosis

1.4.1 Sclerosing Cholangitis

The disruption of the Mdr2 gene in mice is causing an insufficient excretion of phospholipids into the bile canaliculus [22]. Mdr2 (-/-) mice do not show differences regarding growth rate, mortality, weight and external appearance during the first year of age in comparison with wild type mice [23]. At birth, no obvious anatomical changes can be found in the Mdr2 (-/-) [23], however within 2 to 3 weeks of age Mdr2 (-/-) mice do not develop a regular mature phenotype of canaliculi [23]. Livers of Mdr2 (-/-) mice killed 1 day after birth show already alterations to age matched control animals, such as dense neutrophil-granulocytic infiltrate as well as proliferating fibroblasts and a ductular reaction in larger portal tracts [12]. 2 weeks old Mdr 2(-/-) mice shows periductal fibrosis of the onionskin type at medium sized to larger bile ducts[12]. Since histological and macroscopic features found in Mdr2 (-/-) are similar to PSC [12], Mdr2 (-/-) mice represent a suitable model to mimick PSC in mice and is of interest for investigations on the therapeutic impact of substances which are supposed to ameliorate bile composition. Moreover, the model provides the possibility to study mechanisms of inflammation-driven fibrosis [12;23].

1.4.2 Carcinogenesis in Mdr2 (-/-) Mice

Mauad et al. [23] described the progression of the liver disease in Mdr2 (-/-) mice with 129/OlaHsd-genetical background (Harlan UK Limited, UK) as following (Figure 3). After birth the mice are developing nonsuppurative cholangitis, which seems to stabilize after 3 month, between month 4 and month 6 multiple neoplastic tumours start to occur (Figure 3) in the liver of Mdr2 (-/-) mice, accompanied by necrosis and haemorrhage of the tissue, common features of liver cancer. Although α_1-fetoprotein could not be detected multiple mitotic figures, apoptotic bodies as well as atypical hepatocytes and discharged microscopic features were found in Mdr2 (-/-) was suggesting liver cancer appearance [23]. Mauad et al. [23] also describe two animals, which showed nodules in the lung exhibiting catalase positive peroxisomes, which could originate from the liver. Therefore the Mdr2 (-/-) could constitute a well suited model for inflammatory-driven liver cancer. In this regard Pikarsky et al. identified the

nuclear factor kB (NF-kB) in the Mdr2 (-/-) model as an important link between inflammation and tumour development [25]. The group was able to induce apoptosis as well as an interruption of progress to liver cancer. This was accomplished through the inhibition of NF-kB via anti tumour necrosis factor α (TNF-α) treatment as well as using a hepatocyte specific IkB-super-repressor transgene [25]. Thereby they detected NF-kB as a potential modulating factor for cancer development in chronic inflammation [25]. Katzenellenbogen et al. observed in the Mdr2 (-/-) model an induction of anti-inflammatory and antioxidant genes in early stage, a phase where the mitotic activity was still blocked, as well as in late precancerous stages of liver disease [26]. However the less prominent inflammation and the normal antioxidative capacity in late stages of the liver disease did not result in a down regulation of these protective genes. The over-expression of known oncogenes in both stages of liver disease lead to the assumption that the adaptive induced gene expression in the early stage of disease could have effects on the development of liver cancer in later stages of liver disease [26].

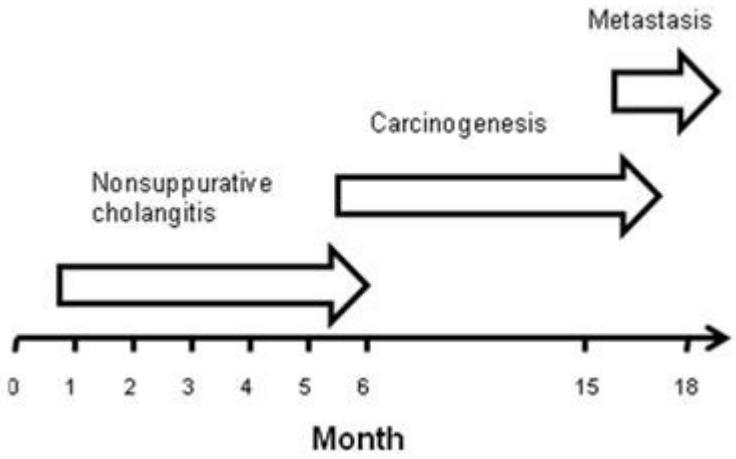

Figure 3: **Course of liver disease in Mdr 2 (-/-) mice. Figure modified after Mauad (Am J Pathol, 1994).**

1.4.3 Gender Differences in Mdr2 (-/-) Mice

van Nieuwkerk et. al. [27] observed gender specific differences in regard to severity of liver pathology in Mdr 2 (-/-) mice and hypothesiszed that the more hydrophobic bile composition in female mice results in a more severe phenotype. As a proof of concept, cholate feeding (0.01% and 0.1% cholic acid supplemented diet) resulted in a loss of gender specificity, while the addition of 0.1% CA induced a dramatic elevation of ALP levels as well as an increase in ALT, Bilirubin and mean histological score. In contrast, feeding of ursodeoxycholate (UDCA) (0.5%) decreased the histological scores and abolished gender differences in the presence of increasing serum ALT levels [28]. Altogether, this set of data indicates that gender differences in Mdr2 (-/-) mice can be modulated by feeding different BAs [27;28].

2 Aims of the Study

The Mdr2 (-/-) mouse model embodies numerous pathological features and characteristics of human SC. Although the Mdr2 (-/-) model is a well established model for inflammatory-driven liver cancer, which takes at least 4 to 6 months to develop neoplastic lesions in the liver [23], not much information about the course of fibrosis after 2 months is available [12].

Therefore we aimed to determine a detailed disease course in this model system and searched for potential gender differences. Of note we aimed to determine whether these animals spontaneously develop cirrhosis.

3 Materials and Methods

3.1 Animals

Frozen serum samples and liver tissue of Mdr2 (-/-) mice at the age between 6 to 13 months were studied retrospectively. Mice were obtained from Jackson Laboratory (Bar Harbor,ME). The mice were fed with a standard mouse diet (Sniff, Soest, Germany), water *ad libitum* and housed with a 12:12 hour light/dark cycle.

3.2 Haematoxylin and Eosin Staining (H&E Stain)

Background:

The H&E staining is a conventional method to stain the nucleus and the cytoplasm in order to make them accessible for light microscopy. The technique is used to mark the basophilic structures with haematoxylin, which results in a purple-blue colour. The eosin is added to stain the eosinophilic structures with a pink colour. The basophilic compounds of the cells are usually nucleic acids, which are located mainly in the nucleus, but can also be found in the ribosome. The eosinophilc formations are typically extra and intracellular proteins [29].

Reagents:

- 4% neutral buffered formaldehyde solution (Merck)
- Paraffin (Vogel)
- Xylol (Merck)
- Haematoxylin solution modified by Gill (Merck)
- 1% Potash alum solution (got from the Apothecary)
- 37% Hydrochloric acid fuming (Merck)
- 0.1% Ammonia solution (got from the Apothecary)
- Eosin Phloxin solution (got from the Apothecary)

- N- butyl acetate (Merck)
- Entellan (Merck)
- Alcohol (100%, 90%, 70% and 50%) (Merck)
- Aqua distillate (Fresenius)

Procedure:

The collected liver tissue of Mdr2 (-/-) mice was fixed in 4% formaldehyde and embedded in paraffin. The 2µm thick sections were prepared by a Microm HM 430 (Zeiss, Germany) microtome. Next the sections were stained with H&E and examined by a pathologist unaware of group arrangement.

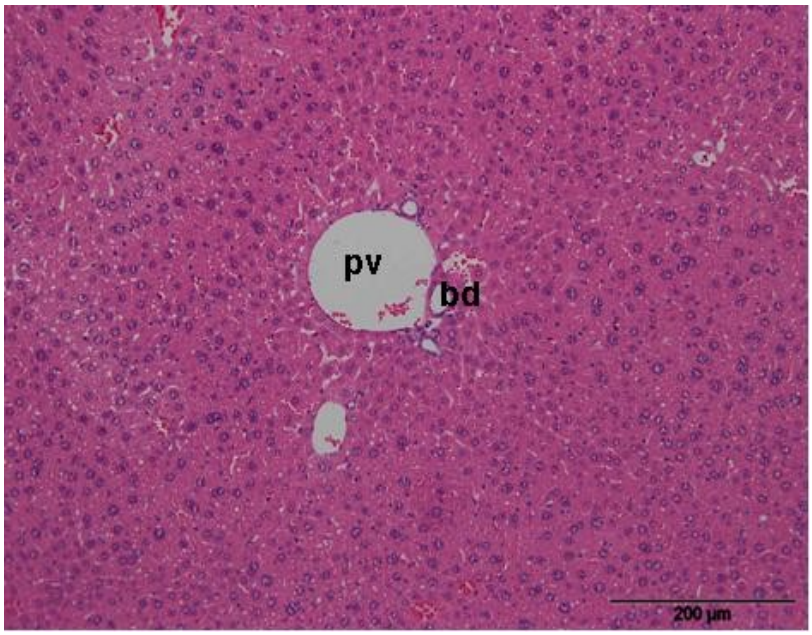

Figure 4: H&E stained normal mouse liver. Basophilic structures (nuclei) take on a purple-blue colour, while eosinophilic intra- and extracellular proteins appear in a pink colour. Portal vein (pv), bile duct (bd); (20x magnification)

3.3 Sirius Red Staining

Background:

Sirius red staining is used to visualize extracellular matrix proteins. This method allows differentiating the collagen, which appears red, from the nuclei (blue), the musculature and the cytoplasm (both yellow). The technique is used to identify connective tissue in diseases, which are associated with features like fibrosis or even cirrhosis. [30]

Reagents:

- 4% neutral buffered formaldehyde solution (Merck)
- Paraffin (Vogel)
- Xylol (Merck)
- Alcohol (100%, 90%, 70% and 50%) (Merck)
- Aqua distillate (Fresenius)
- Entellan (Merck)
- Coelestin-blue (Sigma)
- Iron-alaun solution (got from the Apothecary)
- Picro-Siriusred (0.1% Sirius red in picrinacid-solution got from the Apothecary)
- Haemalaun by Mayer (Roth)
- 0,6% Hydrochloric acid alcohol (Glatt Koller)

Procedure:

Liver tissue of Mdr2 (-/-) mice was fixed in 4%neutral buffered formaldehyde and embedded in paraffin. 2µm thick sections were stained with Sirius red and examined by a pathologist (Cord Langner) unaware of group arrangement.

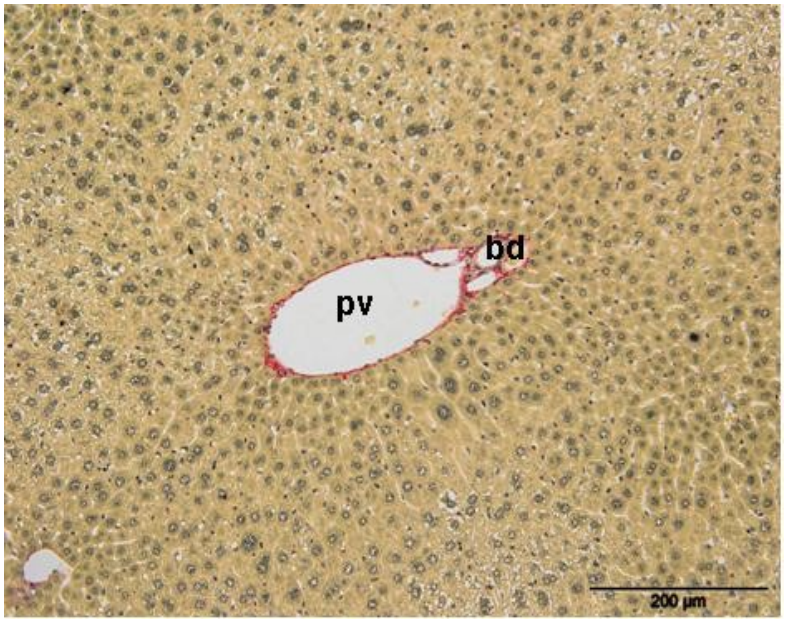

Figure 5: Sirius Red staining of a normal mouse-liver. Connective tissue (collagen-rich) appears red, while cytoplasm is stained yellow and nuclei show a blue colour. Portal vein (pv), bile duct (bd) (20 x magnification)

3.4 Immunohistochemistry

Background:

The principle of immunohistochemistry is the specific binding of an antibody to its antigen on either a frozen or paraffin-embedded tissue. The technique allows localisation or distribution-patterns of the antigen in cells of interest. In addition, changes in expression-levels of antigen can be detected. The visualization of the antibody-antigen reaction is provided by the conjugation of the antibody with an enzyme (for example peroxidase) that catalyses a colour producing reaction making it detectable. [29]

1. Antibody	Species	Dilution	Company	Preservation
Anti Ki67	Rabbit	1:250	Novocastra	Paraffin
Anti α-SMA	Mouse	1:500	Sigma	Paraffin
Anti CK19	Rat	1:500	Hybridoma Bank	Cryo

Table 1: **Antibodies used for immunohistochemistry**

Antigen	Specificity
Ki-67	Marker for mitosis (G1,S,G2)
α-SMA	Marker for activated stellate cells (Myofibroblasts)
CK19	Marker for ductular Proliferation (Cholangiocytes)

Table 2: Antigen and their specificity

Reagents (Paraffin):

- Xylol, 1l (Merck)
- 0,01mol Citrate-Buffer, pH 6,0, 1l (got from the Apothecary)
- Phosphor-Buffered-Saline (PBS got from the Apothecary)
- 30% Hydrogen-Peroxide (H_2O_2), 250ml (Merck)
- Antibody Diluent, 250ml (Dako)
- StreptABComplex/HRP (Dako)
- AEC Substrate Chromogen, 110ml (Dako)
- Haemalaun by Mayer (Roth)
- Microscop Slides: Micro Slides, x-traTM Adhesive (Surgipath)
- Aquatex, 50ml (Merck)
- Dako REAL Envision Detection System, Anti-Mouse, Rabbit Polymer (Dako)
- Monoclonal Mouse Anti α-Smooth Muscle Actin (Sigma) 1:500
- Polyclonal Rabbit Anti Ki67 (Novocastra) 1:250

Reagents (Cryo):

- Phosphor-Buffered-Saline (PBS got from the apothecary)
- Antibody Diluent (Dako)
- StreptABComplex/HRP (Dako)
- AEC Substrate Chromogen (Dako)
- Microscop Slides: Micro Slides, x-traTM Adhesive (Surgipath)
- Aquatexl (Merck)
- 4% neutral buffered formaldehyde (Merck) solution soluted in PBS 1:10
- Methanol (Merck)
- Acetone (Merck)
- Monoclonal Rat Anti-Troma-III (CK19) (Hybridoma Bank) 1:500

Secondary-Antibody (Cryo and Paraffin):

- Polyclonal Rabbit-Anti-Rat Immunglobulins/Biotynilated, 1ml (Dako)
- Multi-Link, Polyclonal Swine: Anti-Goat, Mouse, Rabbit Immunglobulins/Biotinylated, 1ml (Dako)
- Dako REAL Envision Detection System, Anti-Mouse, Rabbit Polymer (Dako)

Procedure:

Immunohistochemistry for Ki-67

Ki-67 immunohistochemistry was performed using the polyclonal rabbit anti-Ki-67 antibody (Novocastra; dilution 1:250) on microwave treated (0.01mmol/L citrate buffer; pH 6.0) paraffin sections. The ABC system with AEC as substrate was used for the detection of antibody antigen binding. The number of positive stained cells was counted per mouse in 20 fields at a 40-fold magnification.

Immunohistochemistry for α-Smooth Muscle Actin (α-Sma)

α-Sma immunohistochemistry was performed on microwave-treated (0.01mmol/L citrate buffer; pH 6.0) paraffin sections. The monoclonal mouse anti-α-Sma antibody (Sigma; dilution 1:500) was used for detection. Binding was detected by using the ABC system with AEC as a substrate.

Immunohistochemistry for Cytokeratin 19 (CK19)

The immunostaining was performed on formol/methanol/acetone fixed cryosections. Therefore the liver sections were fixed for 5 minutes (min) in 4% buffered formalin and afterwards fixed with methanol (5 min at minus 20°C) and acetone (3min at minus 20°C). The anti-Troma-III antibody (Hybridoma Bank; dilutution 1:500) was used for detection of CK19 antigen. The detection was performed using the ABC system with AEC as a substrate.

3.5 Serum Biochemistry

Alanine transaminase (ALT), aspartate transaminase (AST), alkaline phospatase (ALP) and Bilirubin were analyzed by routine clinical chemistry testing performed on a Hitachi 917 analyzer (Boehringer Mannheim, Germany).

3.6 Determination of Hepatic Hydroxyproline Content

Background:

The measurement of hydroxyproline is a method used to quantify collagen content in tissue. Hydroxproline is an amino-acid, which is produced by hydroxylation of proline. The prolyl hydroxylase, represents the responsible enzyme for the reaction and takes place in the lumen of the endoplasmatic reticulum. This process represents a translational modification and plays an important role in endogen collagen production. Since hydroxyproline is found mostly in collagen, the measurement represents a specific method to evaluate the extent of fibrosis. [31]

Reagents:

- Hydrochloric acid (Glatt Koller)
- Filter (Whatman, Schleicher & Schuell)
- Perchloric acid (Merck)
- Hydroxyproline as Standard (Sigma)
- Citrate acetate buffer (ph 6.0)
    - 25g citric acid x H_2O (Merck)
    - 6ml glacial acetic acid (Merck)
    - 60g Na-acetate 3x H_2O (Merck)
    - 17g NaOH (Merck)
    - Ad 500ml aqua distillate (Fresenius)

- 2.2% NaOH in Citrate acetate buffer (Merck)

- Chloramine-T-solution:
  - 0.141g chloramine-T (4°C) (SIGMA)
  - 2ml aqua distillate (Fresenius)
  - 3ml Methoxyethanol (SIGMA)
  - 5ml Citrate acetate buffer

- Dimethylbenzaldehyde-solution:
  - 2g Dimethylbenzaldehyde (4°C) (SIGMA) soluted in 10ml Methoxyethanol (Sigma)

Procedure:

The tissue was homogenized by using hydrochloric-acid, containing 1ml hydrochloric-acid per 50mg liver tissue and incubated for 24 hours at 110°C. The reaction was neutralized by using 2.2% NaOH in citrate acetate buffer. After preparing the samples with chloramine-T-solution, perchloric acid and dimethylbenzaldehyde-solution, the measurement was performed by using a photometer (Eppendorf BioPhotometer, Hamburg) at a wavelength of 565nm.

3.7 Messenger RNA Analysis and Polymerase Chain Reaction (PCR)

3.7.1 RNA Isolation

Reagents:

- Trizol (MRC)
- Chloroform (Merck)
- Isopropanol (Merck)
- Ethanol (Merck)
- MagNA Lyser Green Beads (Roche)

Homogenisation: The hepatic RNA was isolated with TRIzol® (800µl) and homogenized by using the MagNA Lyser Green Beads® system (two times for 20 seconds (sec) at a speed of 6500 rotations per minute).
Separation: For separating RNA from DNA and proteins 160µl chloroform was added to the samples. Then the samples were positioned for 15 min on a rotation plate as well as on a centrifuge (at a speed of 13000 rotations per minute). Finally, the samples were separated into three phases, the lower, which contains a phenol-chloroform phase, an interphase that consists of DNA and proteins and the upper RNA phase.
Precipitation: The RNA (upper phase) was removed into a fresh tube. 500µl isopropanol was added and the samples were centrifuged (at a speed of 13000 rotations per minute) for 15 min.
Washing of RNA: The RNA precipitate was washed with 500µl of 70%-ethanol and centrifuged (at a speed of 13000 rotations per minute) for 15 min.
Dilution of RNA: Finally the ethanol was removed and the pellet was air dried for 5 min. Aqua distillate was added and the tubes were incubated for 10 min at 65°C.

3.7.2 RNA Photometry

RNA photometry (Eppendorf BioPhotometer, Hamburg) was used for measuring the concentration of nucleic acids at a wavelength of 260nm. The zero adjustment was provided by using aqua distillate as a blank. All samples were quantified in duplicates. The purity of the samples was controlled by building the ratio of 260/280nm. This ratio was accepted between 1.4 and 1.8 in order to avoid a protein or phenol contamination.

3.7.3 RNA Electrophoresis

Background:

This method is used to separate the rRNA-molecules by size using an aragose-gel applied at an electric field. The negatively charged rRNA is migrating toward the positive charged anode. Small molecules are able to pass the fine pores of the agarose-gel faster. Therefore this technique allows controlling the quality of the extracted rRNA (28s (Svedberg) and 18s rRNA) in the samples. Ethidiumbromide (a fluorescent dye) is used, in order to make the bands visible under UV–light.

Reagents:

- 3-N-morpholino-propanesulfonic acid (MOPS)-buffer (consisting of 0.2M MOPS, 0.05M sodium-acetate and 0.5M EDTA) (Fluka)
- Sample buffer (consisting of 10ml deionised form-amid, 3.5ml formaldehyde, 2ml 10 x MOPS)
- Loading buffer (consisting of 50% glycerine, 1mM EDTA, 0, 3% bromophenolblue 1mg/ml ethidiumbromide)
- MOPS-gel (consisting of 0,75g Agarose Seakem, 7,5ml 10 x MOPS buffer ad 75ml Aqua distillate.

Procedure:

After photometrical measurement, 1,5µg of the isolated RNA-sample was mixed with 10µl sample-buffer and 3µl loading-buffer following an incubation at 65°C for 10min. The electrophoresis was performed on the 1% agarose-MOPS gel (20 min at 70 Volt).

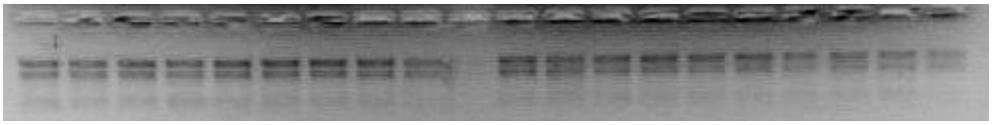

Figure 6: The image shows the 28s and 18s bands under UV-light and verifies the rRNA content and quality of the sample.

3.7.4 Transcription of RNA into cDNA

Background

In order to quantify the RNA amount in further steps using TaqMan® Real Time RT-PCR, it is necessary to use PCR suitable templates. Since RNA cannot be used for PCR, it requires to transcript RNA into cDNA via using a Reverse-Transcriptase. This enzyme enables the synthesis of a DNA strand, which is complementary to the RNA base material. The RNA dependent DNA polymerase needs primers in turn to start transcription. Therefore oligonucleotide complementary to the poly (A9) tail or random hexamer-oligonuceleotides are used. These oligonucleotides usually consist of six random nucleotides. Beside these, also gene specific primers can serve as cDNA transcription template.

Reagents:

- 5x Puffer (Invitrogen 250nM Tris-HCl, pH8.3, 375mM Kcl and 15mM Mgcl2)
- 0.1mol Dithiothreitol (DTT, Invitrogen)
- Deoxynucleotide triphosphats(dNTPs, GeneAmp)
- Superscript TM ll (reverse transcriptase, Invitrogen)
- RNAse inhibitor (Applied Biosystems)
- Random Hexamer (Applied Biosystems)
- Aqua distillate (Fresenius)

Procedure:

A mix of 10µl consisting of aqua distillate with1.5µl RNA and 0.4µl Randomhexamer was used for transcription.
The cDNA as synthesized under temperature cycling conditions, at

- 65° for 5',
- 25° for 10',

after this step the mastermix (containing 4µl 5x buffer, 2µl 0.1M DTT, 0.3µl dNTPs), 0.5µl Superscript Tm ll, 0.5µl RNAse inhibitor and 2.7µl Aqua distillate was added. The cycling was continued at

- 42° for 90',
- 70° for 15'

Finally the cDNA was diluted 1:20 in aqua distillate.

3.7.5 Sybr® Green Real-Time Polymerase Chain Reaction (PCR)

Background:

In this study we used Sybr® green real time PCR, in order to quantify the gene expression of our probes. This technique is based on the use of a non-sequence specific fluorescent agent (Sybr® Green), which binds double stranded DNA. The resulting DNA- Sybr dye emits green light which makes it possible to gather the gene expression from the amount of fluorescent material in the probes at certain points of PCR cycling. The functional principle behind this technique is that through an increase of DNA material the double-strand bound fluorescent dyes signal power is proportionally increasing.

Reagents:

- Sybr® Green PCR Mastermix (Applied Biosystems)
- Primer (MGW BiotechAG)

Procedure:

Gene expression was performed in 20µl reaction mixture containing 5µl diluted cDNA and 15µl Sybr® Green PCR Mastermix (containing of aqua distillate, Sybr Green I dye®, reverse and forward primers). All samples were arranged in duplicates on a 96 well plate.

3.8 Western Blot

Background:

Western blotting is a conventional method to detect and also quantify protein levels in cell extracts. The mechanism is based on an antibody-antigen binding and allows thereby the visualization of proteins. Gel electrophoresis is used to separate proteins, in order to make them more distinguishable. The separation is based on the differentiation of the proteins by their electrophoretic properties (which include the length, molecular weight, the electric charge, the protein folding, posttranslational modifications and other factors). Thereafter the proteins have to be transferred into a medium that makes them accessible for the immunoreactions; therefore a nitrocellulose membrane is used. The proteins are shifted from the gel to the nitrocellulose membrane by electroblotting. After making the prepared proteins accessible for the reaction with the antibodies, they can be detected. Therefore a primary and secondary antibody is necessary. The first is used to mark the specific antigen of interest without binding other membrane proteins. The secondary antibody is needed to bind the species-specific Fc-portion of the primary antibody. It is linked to an enzyme, which visualizes the immunoreactions via luminescence that provides a measurable value [32].

1. Antibody	Company	Dilution	2. Antibody
Monoclonal rat anti-CK19	Hybridoma Bank	1:2500	Dako
Monoclonal mouse anti-αSma	Sigma	1:7500	Dako

Table 3: Antibodies used for Western blotting

3.8.1 Tissue Preparation

Reagents

- Buffer for homogenisation:
  - M Saccharose (Roth);
  - 0.01 Hepes- Caustic potash(Serva);
  - 0.001M Ethylenediaminetetraacetic-acid-disodium-salt-dihydrate (EDTA; Sigma)
  - ad 100µl aqua distillate

- Protease-inhibitor-cocktail (Sigma)

- Phenylmethanesultanylfluoride (Sigma)

- Bradford-reagent:
  - 100mg Blue G-2 (Serva) soltuted in 96% ethanol
  - 100ml 85% orthophosphoric acid (PMSF;Merck)
  - Ad 1l aqua distillate (Fresenius)

Procedure:

50mg liver was prepared and 1ml of the homogenising-buffer, 1µl protease-inhibitor-cocktail plus 1µl PMSF was added to the tissue. After homogenization by using ultrasound three times (for 5 sec.), the samples were stored for 20 min. on ice. Finally, Bradford reagent was added to the supernatant and measured by photometry.

3.8.2 Gel-electrophoresis

Reagents:

- Acryl-amide-solution (30%) 125ml:
    - 37.5g acryl-amide (Fa.BioRad)
    - 1g methylenebisacrylamide (BIS) (Fa.BioRad)
    - diluted in 125ml aqua distillate (Fresenius)

- Separating-gel (=lower gel; 1,5M Tris; 0,4% SDS; pH8.8):
    - 36.3g Tris (Merck) are solute in 50ml aqua distillate 8Fresenius)
    - Setting the pH to 8.8 via using 1N hydrochloric acid (Merck)
    - Adding 0.8g SDS (Fluka) and diluted in 200ml aqua distillate

- Stacking-gel (=upper gel; 0.5M Tris; 0.4% SDS; pH 6.8):
    - 12g Tris (Merck) were solute in 50ml aqua distillate (Fresenius)
    - Setting the pH to 6.8 via using 1N hydrochloric acid (Merck)
    - Adding 0.8g SDS and diluted in 200ml aqua distillate (Fresenius)

- 10x Running buffer 2l:
    - 60g Tris (Merck)
    - 288g glycine (Merck)
    - 20g SDS (Merck)
    - diluted in 2l aqua distillate (Fresenius)

- 1x Running buffer 1600ml:
    - 160ml 10x running buffer
    - filling up to 1600ml with aqua distillate (Fresenius)

- N`-tetramethylenediamine (TEMED) (BioRad)
- Ammonium persulfate (APS) (BioRad)

Procedure:

As gel cassette we used the Mini-PROTEAN® 3 (BIORAD) electrophoresis module. Depending on the molecular size, the right percentage of the separating gel had to be applied. For the detection of α-Smooth muscle antigen (α-SMA) we were using a 10% gel, therefore 2ml of the lowergel was mixed up with 3,3ml aqua distillate and 2,6ml acryl amide solution (30%), filled in a 125ml side-arm vacuum flask and placed under vacuum for 5 min. 50µl ammonium persulfate (APS) and 20µl N`-tetramethylenediamine (TEMED) were added to initiate the polymerisation. The upper gel was prepared of 3ml aqua distillate, 0.75ml acryl-amide solution (30%) 1.25ml stacking-gel solution. The mixture was also de-aerated via using a vacuum pump. As described above the polymerisation was initiated by adding 20µl ammonium persulfate (APS) and 15µl N`-tetramethylenediamine (TEMED). In the interval the aqua distillate was decanted and exhausted using a filter paper. The cassette was filled with the stacking gel and a comb was used to create the slots for the samples. After one hour the gel was fully polymerized, the comb was removed and the slots were filled up with the 1x running buffer. While the first slot was loaded with 7µl of a standardized 10kDa protein (Gibco®, Life Technologies) the other are loaded with the protein samples. Finally the samples were running into the gel about 200V for 5 min., after which the voltage is lowered to 100V for about 1 hour.

3.8.3 Transfer (Electroblotting)

Reagents:

Transfer Buffer:

- 7g Tris (Merck)
- 35.75g glycine (Merck)
- diluted in 2l aqua distillate (Fresenius) and 500ml methanol (Merck)

Procedure:

A transfer sandwich was created, in order to mediate the translocation of the proteins from the gel to the membrane. The formation therefore was arranged as follows:

- Cathode
- Transfer buffer soaked sponge
- 2 layers of filter paper
- gel, nitrocellulose membrane
- 2 layers of filter paper
- Transfer buffer soaked sponge
- Anode

The transfer sandwich was placed in the transfer tank and the proteins were transferred for 2 hours at 100V.

3.8.4 Blocking of Membrane

Reagents

- PonceauS (Fluka)

- 1x TBS-T 0.1%Tween: (Merck)
    - 100ml 10xTBS plus 1mlTween are filled up 1l with aqua distillate

- Blocking buffer:
    - 5% non-fat dried milk (Merck)
    - 0.1% Tween 20 (Merck)
    - ad 1l Tris (Merck)

Aqua distillate (Fresenius)

Procedure

The membrane was stained using PonceauS. After marking the region, the membrane was trimmed and flushed with aqua distillate,TBS-T and finally blocked in 5% non – fat dried milk for at least an hour or over night at 4°C.

3.8.5 Immunoreaction and Detection

Reagents:

- 1x TBS-T 0.1% Tween:
    - 100ml 10xTBS plus 1ml Tween are filled up 1l with aqua distillate
- 5% non-fat dried milk in TBS-T
- Monoclonal Rat-Anti-CK19 antibody (Hybridoma Bank) 1:2500
- Monoclonal Mouse-Anti-αSma antibody (Sigma) 1:7500
- Secondary antibody (Dako)
- ECL Plus Western blotting Detection System (GE Healthcare)
- Film (Kodak XDA Plus)

Procedure:

After the proteins were transferred to the nitrocellulose membrane, a monoclonal mouse antibody against αSma (Sigma; dilution 1:7500) and a monoclonal rat anti CK19 (Hybridoma;dilution 1:2500) were used for blotting. The binding was detected with a peroxidise-conjugated rabbit immunoglobulin against mouse and rat Fc-portion (Dako). The peroxidise activity was visualized by using the ECL system

3.9 Statistical Analysis

Three to seven animals were studied at each point of time. We used the Mann-Whitney-U test, which represents a non parametric test to compare two independent samples. A p value lower than 0.05 was considered as statistical significant.

4 Results

4.1 Serum Biochemistry and Cell Proliferation

4.1.1 Serum Biochemistry

No age or sex dependent differences were observed in regard to changes in serum-biochemical parameters (Figure 7). However, male mice tended to show lower levels of ALT, AST and ALP (black columns) which however did not reach statistical significance.

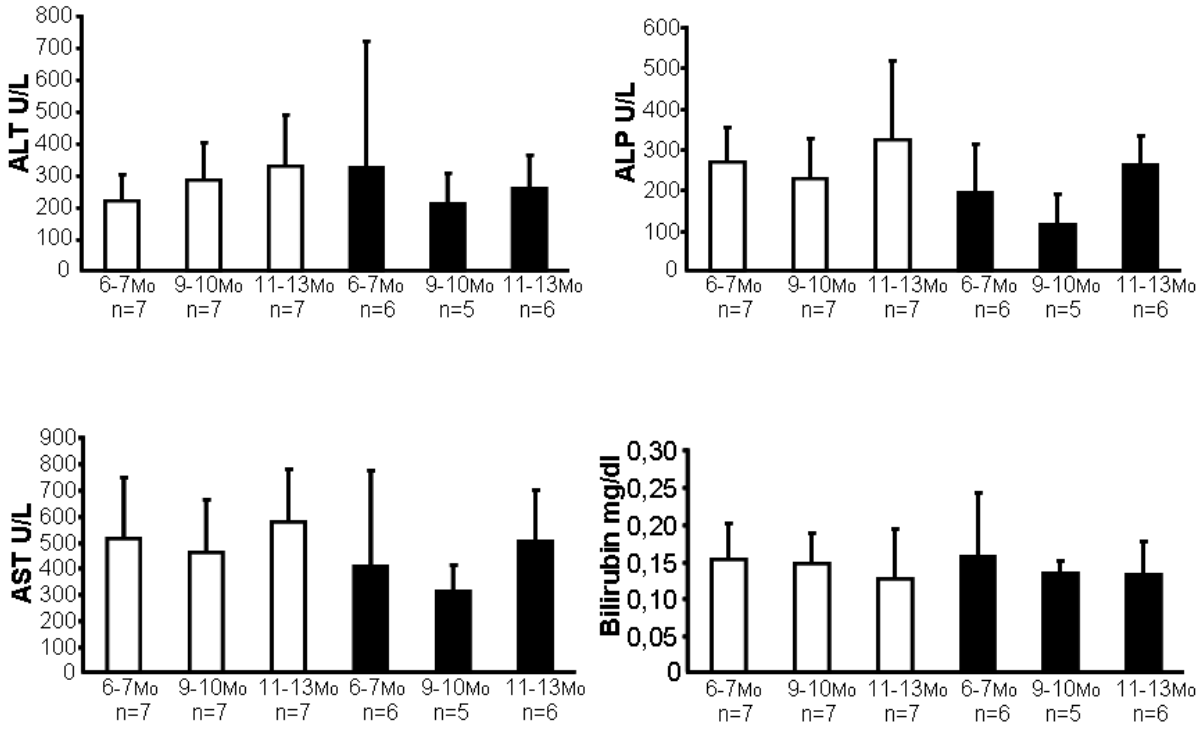

Figure 7: Serum ALT, AST, ALP and bilirubin levels in female (open bars) and male mice (closed bars) at different age.

4.1.2 Cellular Proliferation Reflected by Ki-67 Positive Cells

In order to investigate the proliferative status of hepatocytes, we used immunohistochemical staining of Ki-67 antigen and subsequently counted the number of positive stained cells per mouse in 20 fields at a 40-fold magnification. Figure 8 shows the average of the positive hepatocytes per field and group. No significant changes were observed between the different groups.

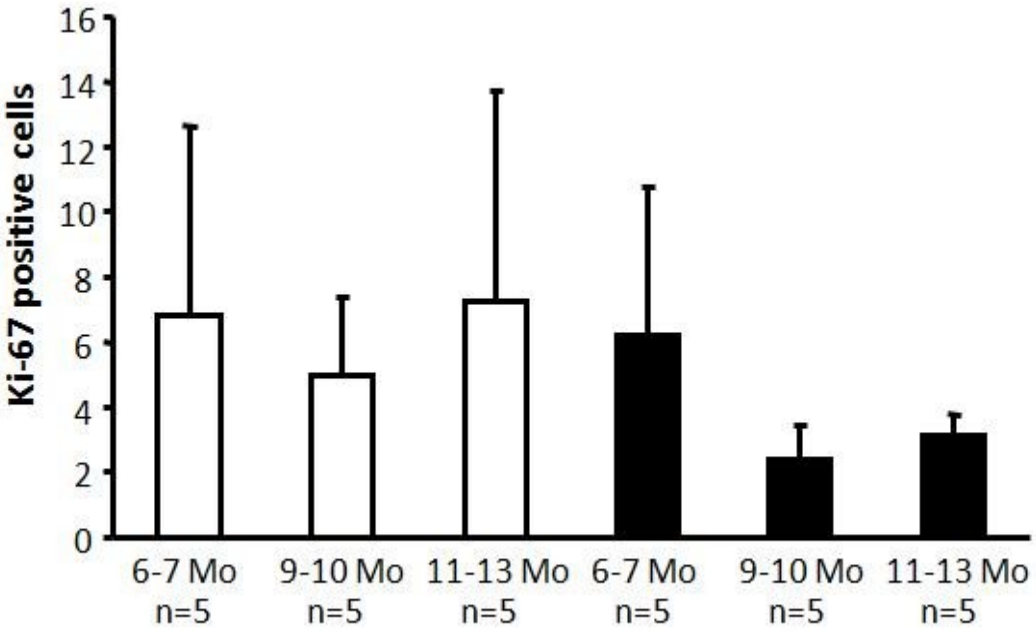

Figure 8: Average of Ki-67-positive hepatocytes per field and group counted at a 40-fold magnification in 20 fields per mouse (open bars female; closed bars male).

4.2 Fibrosis

4.2.1 Sirius Red Staining

Fibrotic tissue content increased over time (Figure 9). Interestingly, female mice showed a more severe phenotype characterized by portal field fibrosis, while the lobular fibrosis remained constant over time and did not show gender differences (Figure 10).

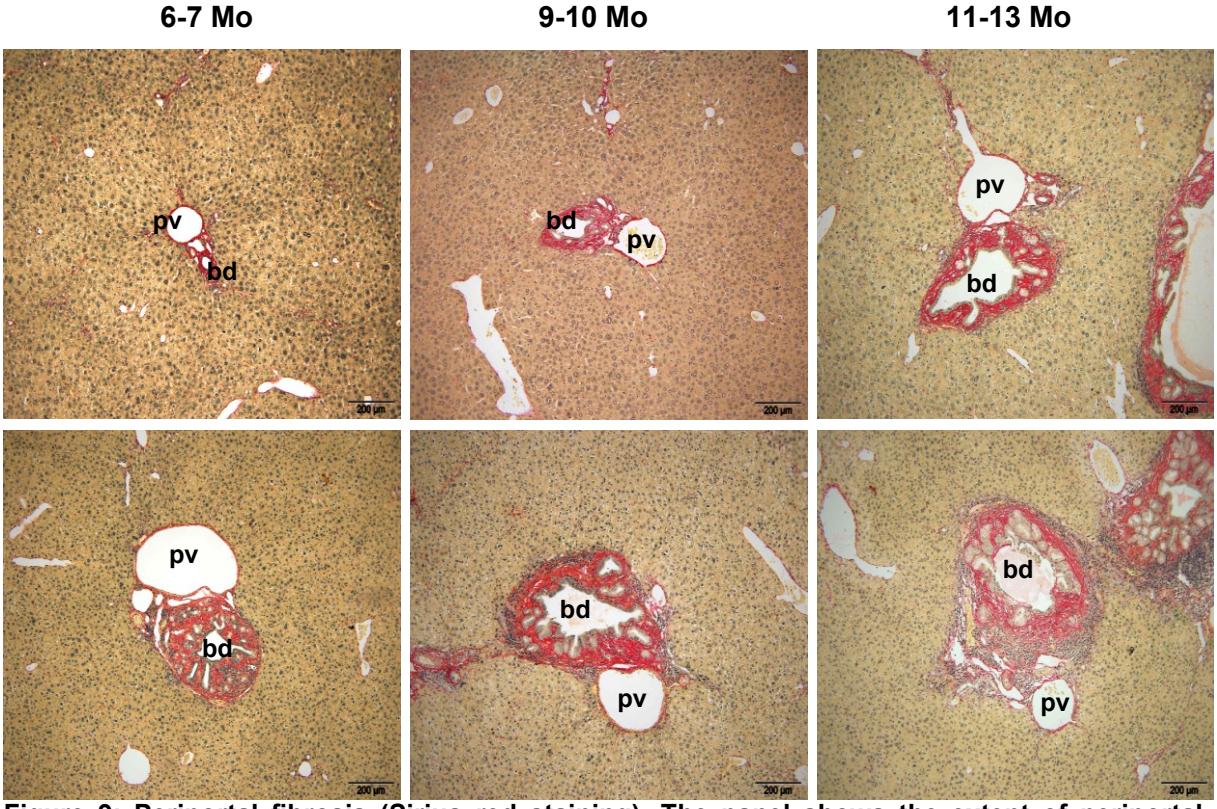

Figure 9: Periportal fibrosis (Sirius red staining). The panel shows the extent of periportal fibrosis in the different groups (upper panels male; lower panels female). Female mice show a higher extent of periportal fibrosis. Portal vein (pv), bile duct (bd). (10x magnification)

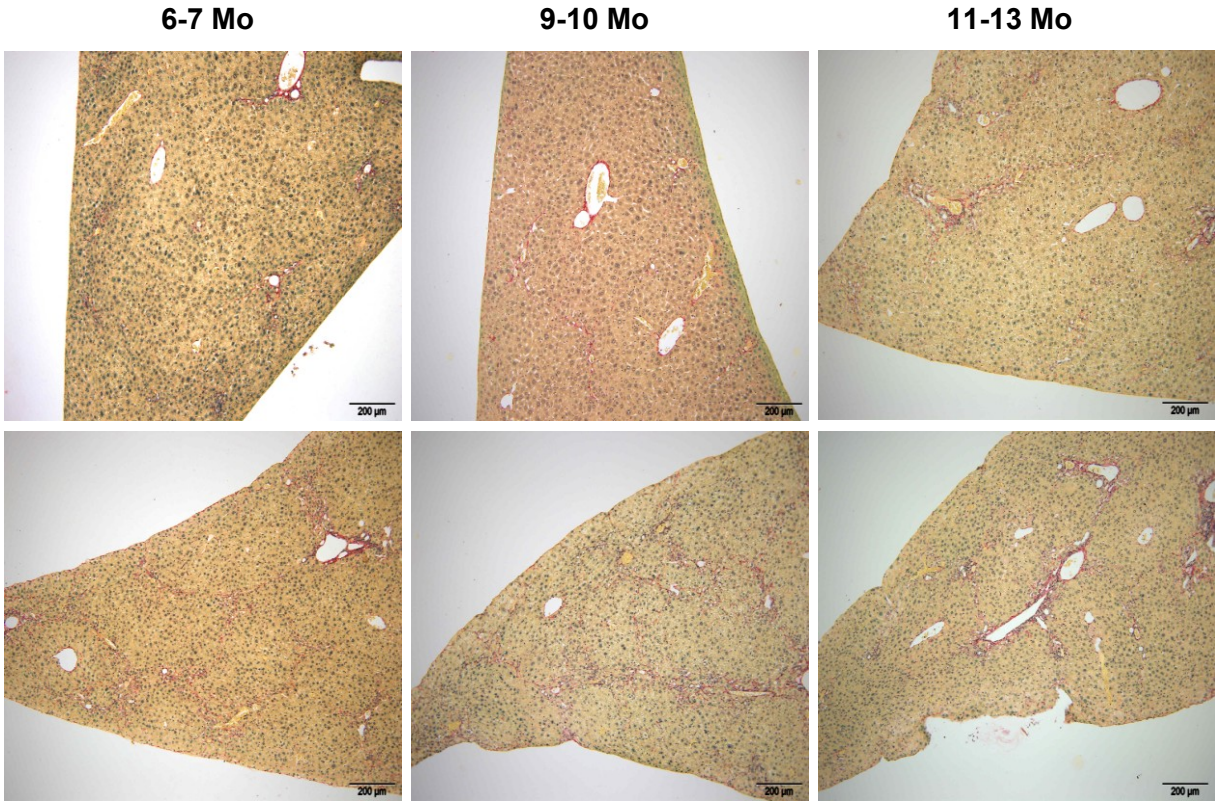

Figure 10: Lobular phenotype (Sirius red staining). No differences in lobular fibrosis (upper panels male; lower panels female). (10x magnification)

4.2.2 Hydroxyproline Content

As shown in Figure 12, the average of hydroxyproline content (microgram per gram of liver) was statistically higher between 6 to 7 month, as well as 9 to 10 month-old female and male. The last time point did not reach significance because of the limited amount of animals in the male group (n=3).

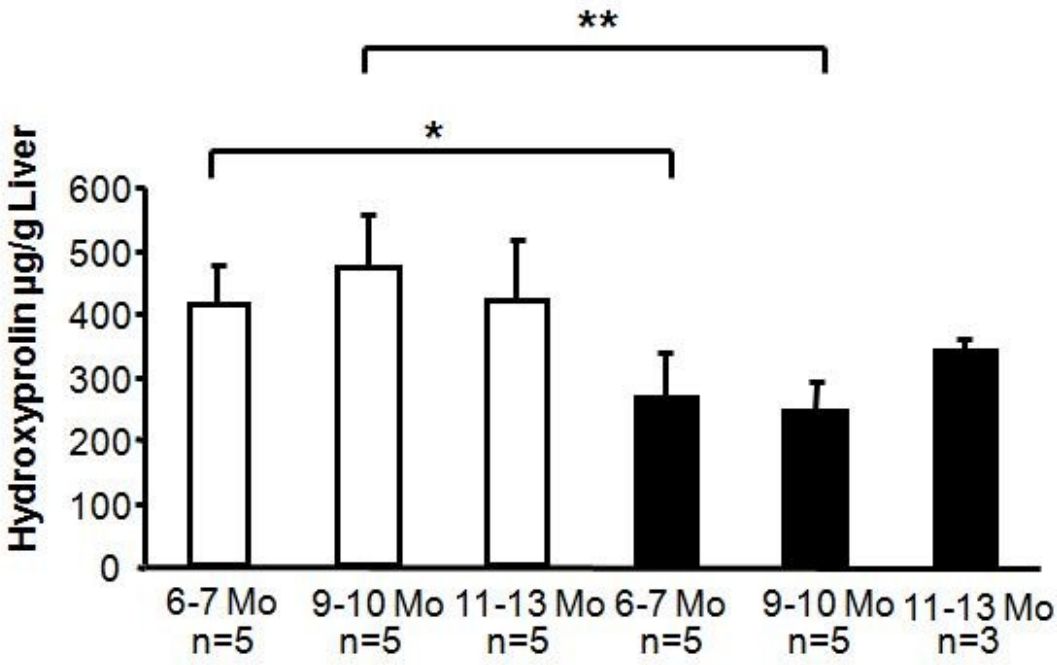

Figure 11: Hydroxyproline measurement. 6-7 month old groups female vs. male ($p<0.05$; *) , 9-10 month groups female vs. male ($p<0.01$;) (open column female; black column male).**

4.2.3 α-Sma Immunohistochemistry

Immunohistochemistry of α-Sma antigen (Figure 12) showed a pronounced staining of positive cells at the large ducts, but no gender differences in regard to distribution or amount of staining. However, while α-Sma protein expression in female mice - measured via Western Blot- seemed to be constant over time (Figure 13); male animals showed a lower but ascending amount of protein expression during the course of the disease (Figure 12). No positive cells were found in the lobule.

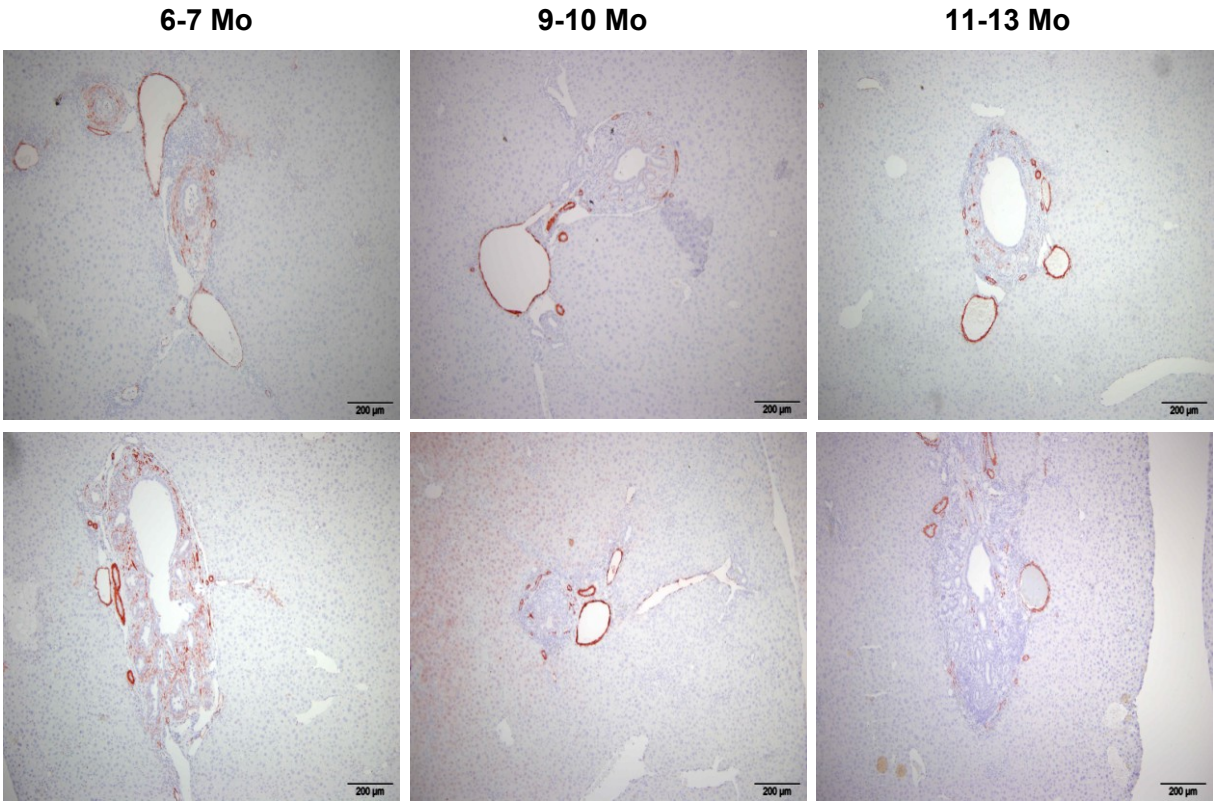

Figure 12: α-Sma immunohistochemistry. The panel illustrates the staining of α-Sma positive cells at the portal fields. No gender differences in regard to amount or distribution were observed (upper panel male; lower panel female).

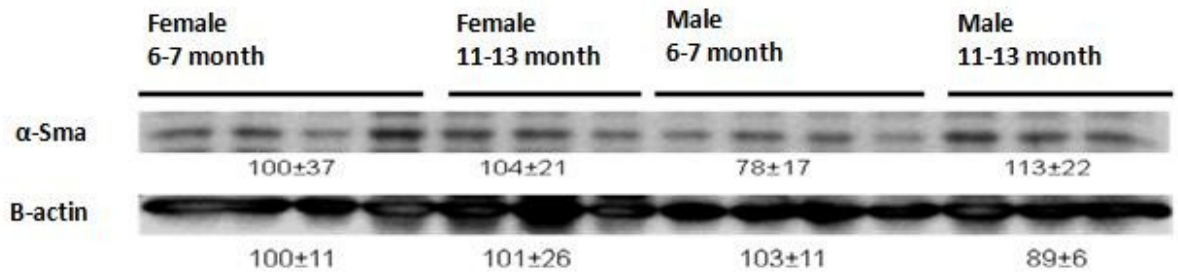

Figure 13: Western blot analysis of α-Sma protein. The mean value and standard deviations of the adjusted volume are normalized on the 6-7month old female group. No significant changes were observed. B-actin was used as a control.

4.2.4 Fibrosis Gene Expression

Figure 15 shows the expression of the fibrosis relevant genes normalized on 18s RNA, which was used as housekeeping gene. No gender differences between the groups and no changes over the course of the development were observed. Collagen type 1 alpha 1 (Col1a1), the profibrolytic matrix metalloproteinase 13 (Mmp13) and the profibrogenic tissue inhibitor of metalloproteinases 1 (Timp) showed a constant expression over the course of the disease. Taken together, these results suggest that fibrogenesis turnover was no modified at these points of time.

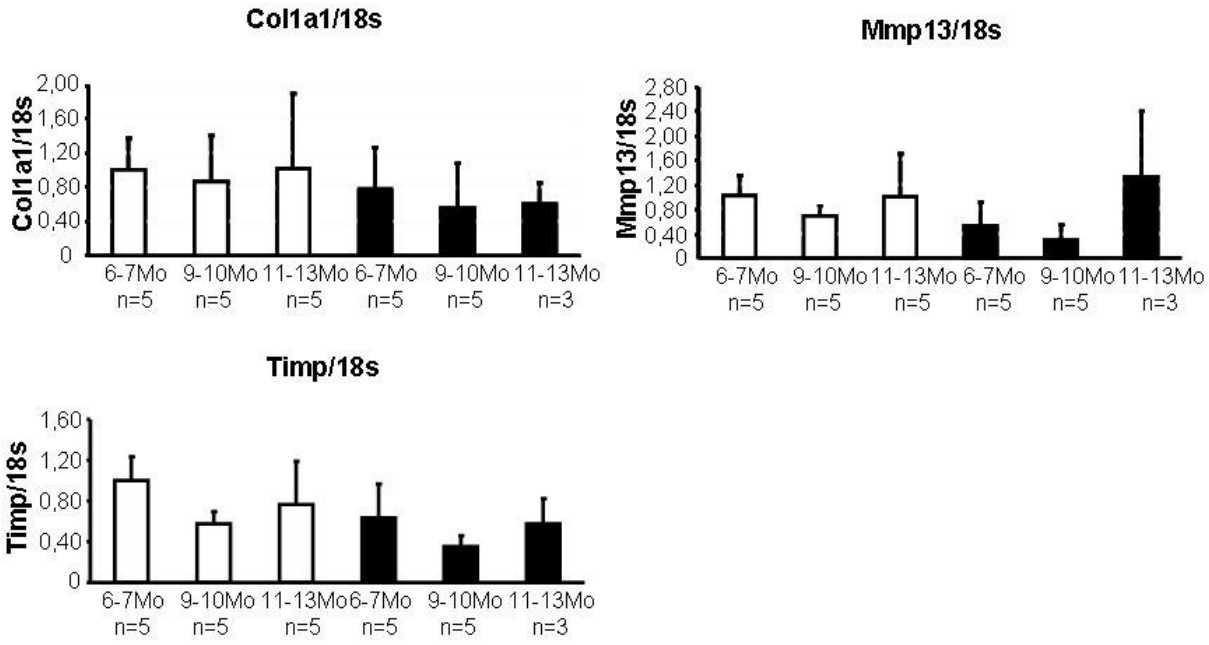

Figure 14: mRNA expression of fibrosis relevant genes. No statistically significant differences were observed. However the expression of collagen stays constant, the genes reflecting the turnover of collagen show parallel variations at the different points of time (open bars female; closed bars male).

4.2.5 Do Mdr2 (-/-) Mice Develop Liver Cirrhosis?

Until month 13 no liver cirrhosis could be observed after H&E staining. Although some signs of biliary type of liver damage were detected such as cholate stasis, no full blown histological features of cirrhosis like regenerative nodules, or marked deposition of connective tissue between the lobules or sever (cirrhosis-like) changes of liver architecture, were found (Figure 15).

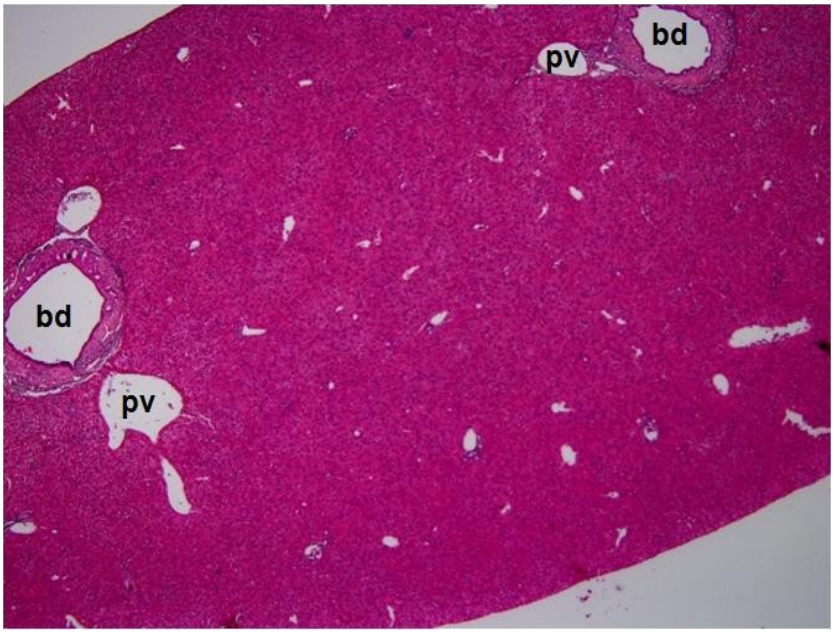

Figure 15: H&E sections of 13 month old mice; No regenerative nodules, marked deposition of connective tissue or severe changes of liver architecture were observable. No evidence for liver cirrhosis detected. (4x magnification)

4.3 Inflammation

The expression of Monocyte chemotactic protein-1(Mcp-1) was constant over time, whereas the macrophage marker F4/80 was significantly lower ($p<0.01$) in the 9 to 10 month old male group compared to the same aged female group. Furthermore, interleukin-1β (IL-1β) gene expression was elevated in the 9 to 10 month old female group compared to their male counterparts ($p<0.01$) (Figure 16). Since inflammation can drive fibrogenesis, these results are suggesting that the more limited fibrogenesis found in males (Figure 16) could be due to less inflammation.

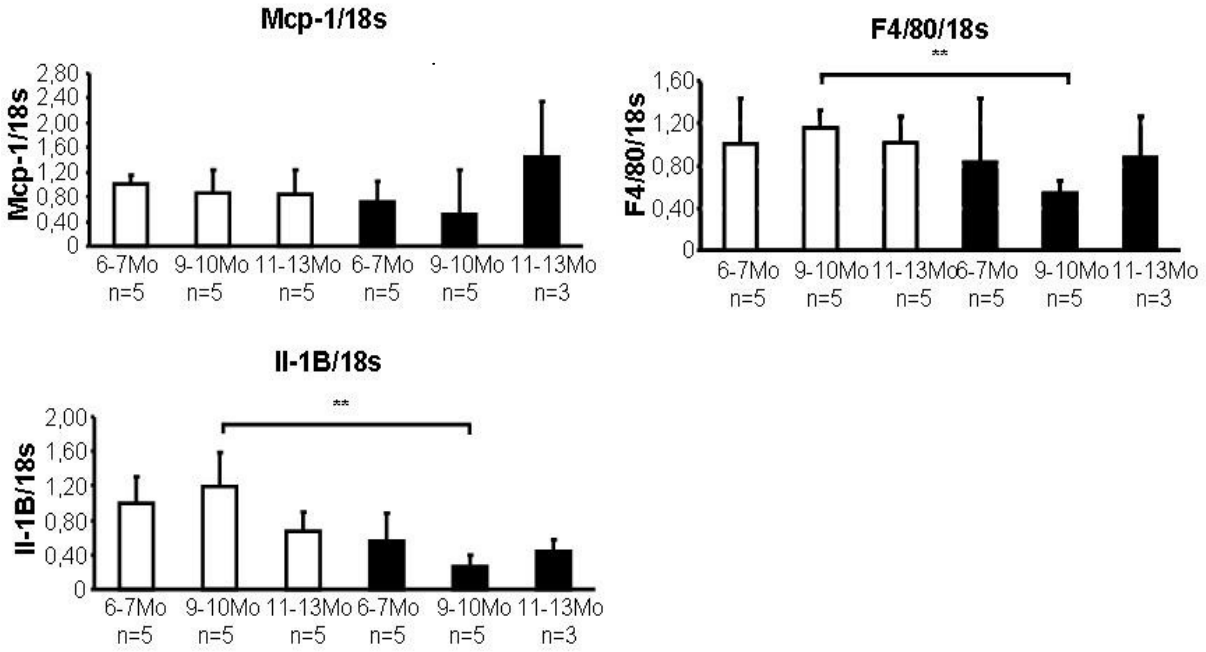

Figure 16: mRNA expression of inflammation relevant genes. Inflammatory genes in male mice are expressed at a significant lower level at the second point of time with respect to interleukin-1β ($p<0.01$) and F4/80 ($p<0.01$) gene expression. All genes were normalized (open bars female; closed bars male).

4.4 Ductular Proliferation

We next investigated the expression of CK19 mRNA, protein (Western Blot) and staining. CK19 immunohistochemistry (Figure 17) and protein levels (Figure 18) remained constant over time. However, Ck 19 mRNA showed a significantly higher expression at the first time point (6-7 month) in female mice ($p<0.01$) (Figure 19). Therefore, we can conclude that post-transcriptional mechanisms kept CK19 protein expression constant and that ductular proliferation was not changed in a sex-specific manner.

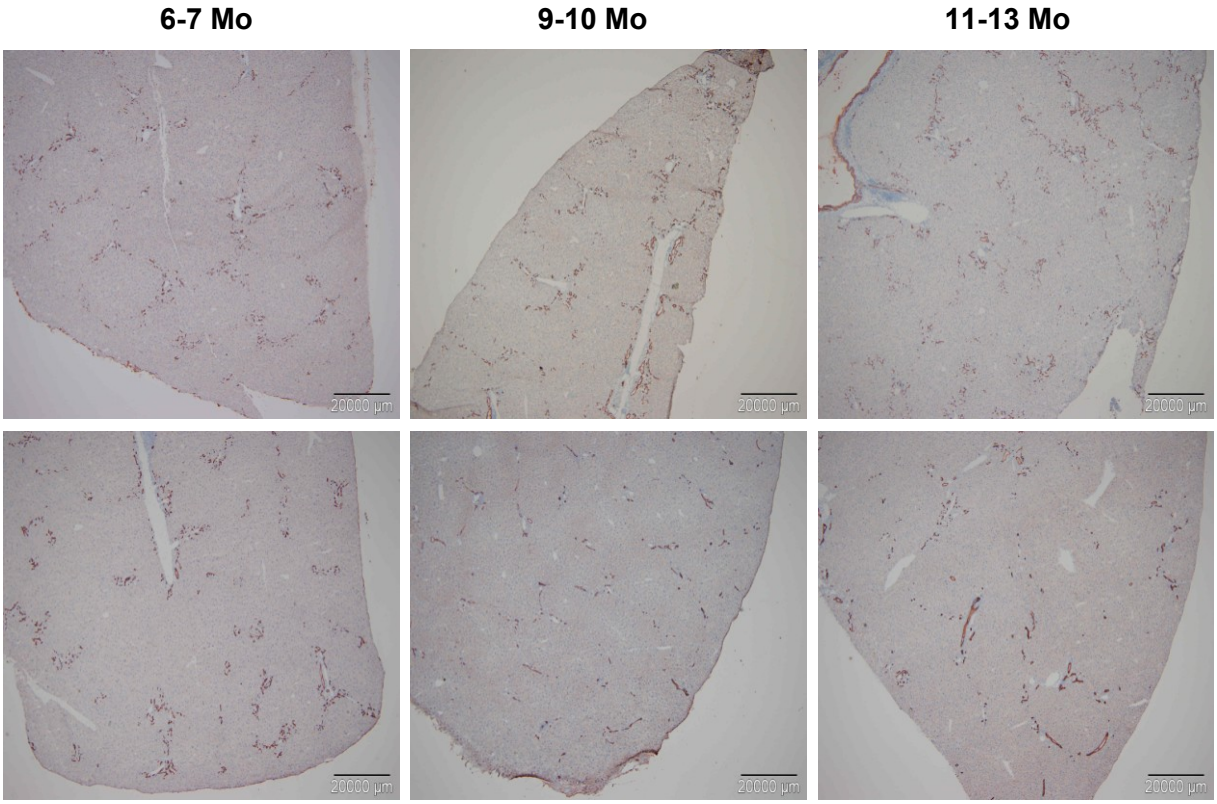

Figure 17: CK19 immunohistochemistry. The immunohistochemical staining of CK19 resulted in no impressive distinctions in amount as well as distribution of the antigen and thereby leads to the impression of a constant phenotype in regard of ductular proliferation.

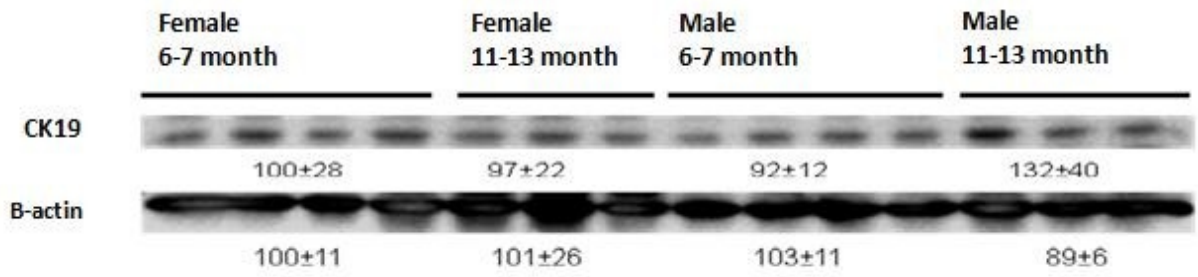

Figure 18: Western blot analysis of CK19 protein. The mean value and standard deviations of the adjusted volume are normalized on the 6-7month old female group. No significant changes were observed. B-actin was used as a control.

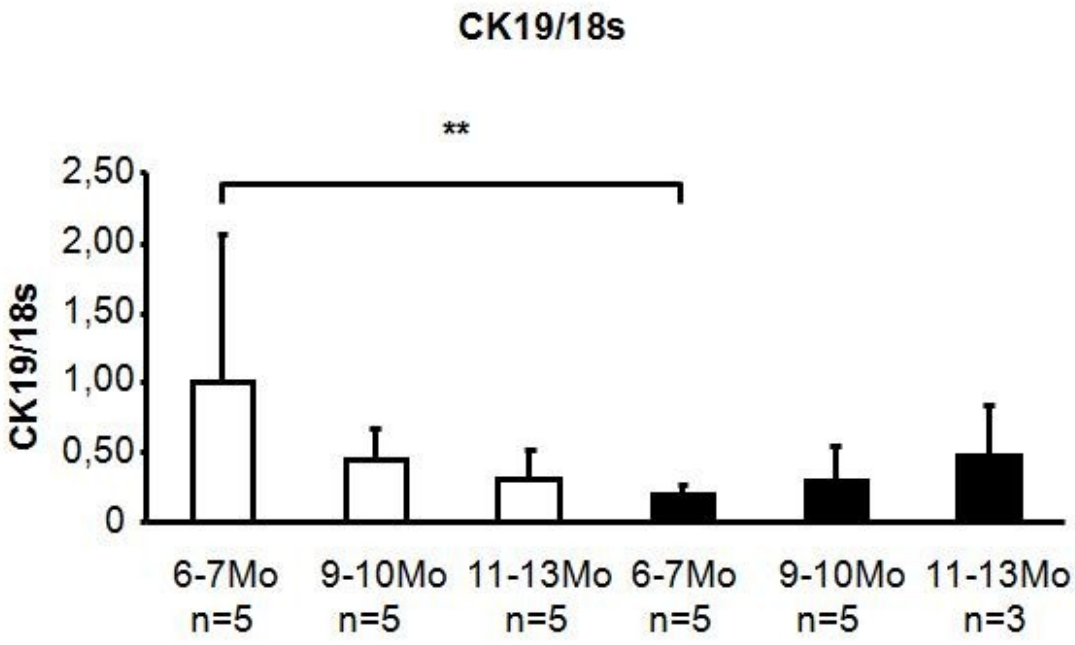

Figure 19: CK19mRNA expression. Male mice showed a lower CK19 gene expression at an age of 6 to 7 months compared to the female animals ($p<0.01$). The gene expression was normalized on 18 sRNA (open bars female; closed bars male).

5 Discussion

The Mdr2 (-/-) represents a well-characterized model for sclerosing cholangitis and mimics several key morphological aspects of PSC [12;24]. Since the etiopathogenisis of sclerosing cholangitis is still poorly understood, this model represents an attractive approach to investigate potential underlyining disease mechanisms. A better understanding of the basic pathogenetic mechanisms of chronic immune mediated cholangiopathies is essential for developing new diagnostic, prognostic as well as therapeutic tools for these disorders.

Several rodent models for chronic immune-mediated cholangiopathies such as PSC are available. Unfortunately to date no animal model exhibits all features of PSC [33;34]. Models which are induced by bacterial cell components or colitis fill the gap of the association between IBD and cholangiopathies [34]. Drugs or xenobiotics induced bile duct injury, via 3,5-diethoxycarbonyl-1,4-dihydrocollidine or litocholic acid, lead to biliary fibrosis or even cirrhosis through a direct toxic or immune-mediated injury [34]. Interestingly cystic fibrosis transmembrane conductance regulator (Cftr) knockout mice develop liver injury with features of hepatosteatosis, focal cholangitis, inspissated secretions, bile duct proliferation and progression to focal biliary cirrhosis after 1 year of age, possibly through an impairment of hydration and alkalinization of bile [34].

The Mdr2(-/-) model develops pericholangitis, periductal fibrosis with ductular proliferation and finally sclerosing cholangitis, because of a disrupted phospholipid excretion. This defect results in an increase of free non-micellar bile acids and a more hydrophobic “toxic” bile [11;12;13,34]. As a consequence mice are developing histological changes resembling human PSC. This makes it the most valuable knockout-model for this type of cholestatic disorder. Since there is an urgent need for new medical treatment strategies in human PSC, this model has often been chosen as an approach for testing novel therapeutics.

Interestingly the reported date in literature in regard to gender-differences of liver fibrosis in diverse chronic liver diseases are conflicting [35]. The fibrosis progression in female is slower compared with male in chronic hepatitis C,

whereas female, who are suffering from alcoholic liver disease progress to liver fibrosis more rapidly [35]. This controversy is probably related on the one hand to the inhibiting effects of estrogens on the proliferation of stellate cells in chronic hepatitis C but on the other hand due to a smaller distribution volume and a lower activity of gastric dehydrogenase in female suffering from alcoholic liver disease [35;36;37;38]. C. M. van Nieuwkerk [27;28] observed a significantly different phenotype between male and female animals and accounted this finding to a different bile composition [27]. She was able to assimilate the phenotypes between sexes via nutritional bile feeding [28]. Furthermore, some data revealed a higher susceptibility for female Mdr2(-/-) mice to develop cholecysto- and hepatolithiasis [39]. Lammert et. al. [39] showed in this study, that female mice display a more hydrophobobic bile-content because of lower tauro-β-muricholate levels and sees thereby a rational to substitute patients who are suffering from LPAC with UDCA in order to create a more hydrophilic BA-pool. Therefore we focused on possible gender differences as well as the time course in the development of the disease phenotye in the Mdr2 (-/-) mode

Data on the time course of the development of sclerosing cholangitis is scarce. The current opinion is that in this model the phenotype is already fully established at 2 months of age [12]. Therefore it is used to start at this point with the administration of novel therapeutic substances. However, it is not yet been firmly established whether the cholangitis progresses any further or regresses beyond this time point, although it has been shown that these animals develop HCC presumably via continued underlying liver pathology. Therefore we studied the unknown course of cholangiopathy after 2 months in regard to the time course as well as possible gender differences.

We were able to describe the course of liver disease in aspects, which are unknown and also controversial to previous findings. Maud et al. [23] published the observation of multiple tumours already after 4 to 6 months in the Mdr2 (-/-) model. This finding cannot be confirmed by our study, since there were still no neoplastic lesions at 13 months of age. Anyhow this finding can be due to, since these studies were performed in mice with a 129/OlaHsd-genetical background, while we used FVB-genetic background. Furthermore the group described hepatocellular lesions in their study. Although patients who are suffering from

PSC normally develop cholangiocellular carcinomas (CCC), they also have a higher risk of developing hepatocellular carcinoma development [40;41;42]. So this model covers an important attribute also found in PSC namely the higher susceptibility for inflammation driven carcinogenesis.

Significant sex-differences could be observed in hydroxyproline liver content (Figure 11), CK19 (Figure 19) and IL-1β mRNA (Figure 16) expression in the first age-bracket as well as distinctive mRNA levels of F4/80 (Figure 17) at the second age-bracket in regard of sex differences. However differences often missed reaching statistical significance marginally, which may be due to the low number of available animals and inhomogeneity of the groups. In most of our findings gender-differences were observable by trend, which shows within a constant but more severe phenotype in females, while males show a lower ascending course of disease after 2 months of age.

Most importantly we did not observe liver cirrhosis until 13 months of age. This finding is contrary to the course of human PSC, which commonly results in liver cirrhosis. Anyhow characteristic features of histological biliary liver damage like cholate stasis were detected but did not increase in severity any further from month 6 until month 13 and did not show progression to liver cirrhosis. This finding raises the question, whether cirrhosis occurs at a later point of time or if the mice do not progress to liver cirrhosis, which could be due to a possible less toxic bile acid-pool in mice in comparison to human.
The hydroxyproline measurement showed a significantly lower level in male mice (Figure 11), which appears in an ascending nature over the time course. In contrast female mice showed a constant amount of hydroxyproline over time. Accordingly the α-Sma immunohistochemistry (Figure 12) also showed a constant expression in females, while it increases in males over time. Since α-Sma (+) myofibroblasts are recognized as fibrogenic and mainly responsible for liver fibrosis via deposition of collagen type 1 [43], this finding is in agreement with findings in hydroxyproline measurement. On the one hand this observation gives the impression, that a certain content of fibrotic tissue surrounding the injured ducts may be necessary in order to stop disease progression to cirrhosis. This phenomenon could result from a sufficient isolation of liver tissue against toxic monomeric BAs and thereby in an autonomous

stabilization. On the other hand this finding raises the question why there was no improvement of markers in regard to liver function, fibrosis, inflammation or ductular proliferation after a possible duct ‘insulation’.

The occurring sex differences in regard to extent of fibrotic tissue could appear due to different bile composition, since van Nieuwkerk et. al. described a more severe phenotype in females caused by more hydrophobic bile content [27], which was underlined also by the findings of Lammert et. al. [39]. The toxic non micellar bound BAs could act as a stimulus for fibrogenesis and could thereby result in a later necessity for isolation in males, because of a less hydrophobic and thereby a less toxic bile contribution.

Nevertheless this assumption is very speculative and further studies, which include the collection of bile at different points in time, have to be performed. Furthermore a treatment with fluorescent UDCA in Mdr2 (-/-) mice, as performed by Fickert et. al [24], after 2 months has to be considered. The lack of labelled UDCA in the periportal hepatocytes could underline a sufficient isolation.

Inflammation with leukocytes and cytokine release are known triggers of hepatic fibrosis [44]. In our study we observed a difference in expression of inflammation related genes between males and females. A statistical-significantly lower level of F4/80 and Il-1β was observed in male mice. This could reflect a further reason for a lower amount of liver fibrosis in males.
The findings of our study suggest some kind of stabilization in regard of liver injury, which is underlined by the missing development of cirrhosis, a stabled liver function as well as fibrosis, inflammation and ductular proliferation relevant markers. Gender differences point to a later stabilization in male mice, which do not show the same severe phenotype as well as fibrotic status after six months.

There are several limitations to our investigation. The number of available mice was low and was responsible for considerable inhomogeneity, caused by the different generations of knockout mice. Furthermore no bile was available, which prevents the examination of bile composition over time in terms of associated development of bile

duct injury and a possible explanation for the missed cirrhosis since the BA-pool in mice over time is unknown.

Further studies have to be performed in order to identify the reason for the lack of progression of the cholestatic liver injury, since this could help to identify possible disease modulating factors in human cholastatic disorders.

6 References

[1] : Horn F., Moc I., Schneider N., Grillhösl C., Berghold S., Lindenmeier G. (2005) “Biochemie des Menschen” Georg Thieme Verlag KG, Stuttgard, Germany

[2] : Trauner M., P.J. Meier and J.L. Boyer (1998) “ Molecular pathogenisis of cholestatsis.” N Engl J Med 339(17): 1217-1227

[3] : Geier A., Wagner M., Dietrich C.G., Trauner M.(2007). “Principles of hepatic organic anion transporter regulation during cholestasis, inflammation and liver regeneration” Biochim Biophys Acta. 1773(3):283-308

[4] : Jones P.M. and George A.M. (2004). "The ABC transporter structure and mechanism: perspectives on recent research". Cell Mol Life Sci. **61** (6): 682–99

[5] : Russel D.W. and K.D. Setchell (1992) “Bile acid biosynthesis.” Biochemistry 31(20):4737-4749

[6] : Hofmann A.F., Hagey L.R., (1998) “Bile acids and biliary disease: peaceful coexistence versus deadly warfare.” Gut and Liver : 85-103

[7] : Hofman A.F. (1999) “The continuing importance of bile acids in liver and intestinal disease.” Arch Intern Med 159(22): 2647-2658

[8] : *Thomas C., Pellicciari R., Pruzanski M., Auwerx J., Schoonjans K.* (2008) “Targeting bile-acid signaling for metabolic diseases” Nat Rev Drug Discov. 7(8):678-93

[9] : Gadaleta R.M., van Mil S.W.C., Oldenburg B., Siersema P.D., Klomp L.W.J., K.J. van Erpecum “Bile acids and their nuclear receptor FXR: Relevance for hepatobiliary and gastrointestinal disease” (2010) Biochim Biophys Acta. 1801(7):683-692

[10] : Elferink R.P., Tytgat G.N., Groen A.K. (1997) “Hepatic canalicular membrane 1: The role of mdr2 P-glykoprotein in hepatobiliary lipid transport” FASEB J. 11(1):19-28

[11] : Smit J.J.M., Schinkel A.H., Oude Elferink, Groen A.K. Wagenaar E., et al. (1993) “Homozygous Disruption of the Murine mdr2 P-Glycoprotein Gene Leads to a Complete Absence of Phospholipid from Bile and to Liver Disease” Cell. 1993 Nov 5;75(3):451-62

[12] : Fickert P., Zollner G. Fuchsbichler A., Stumptner C., Weiglein A.H., Lammert F., Marschall H.U., Tsybrovskyy O., Zatloukal K., Denk H., Trauner M. (2002) “Ursodeoxycholic acid aggravates bile infarcts in bile duct-ligated and Mdr2 knockout mice via disruption of cholangioles.” Gastroenterology 123: 1238–1251.

[13] : Trauner M., Fickert P., Halilbasic E., Moustafa T. (2008) “Lessons from the toxic bile concept for the pathogenesis and treatment of cholestatic liver diseases” Wien Med Wochenschr. 158(19-20): 542-8

[14] : Zollner G., Wagner M., Trauner M. (2010). “Nuclear receptors as drug targets in cholestasis and drug-induced hepatoxicity” Pharmacol Ther. [Epub ahead of print]

[15] : Lang C., Meier Y., Stieger B., Beuers U., Lang T., Kerb R., Kullak-Ublick G.A., Meier P.J., Pauli-Magnus C. (2006). “Mutations and polymorphisms in the bile salt export pump and the multidrug resistance protein 3 associated with drug-induced liver injury.” Pharmacogenet Genomics 17(1): 47-60

[16] : Trauner M., Fickert P., Wagner M. (2007). “MDR3 (ABCB4) defects: a paradigm for the genetics of adult cholestatic syndroms.” Semin Liver Dis. 27(1): 77-98

[17] : Melum E., Boberg K.M., Franke A., Bergquist A., Hampe J., Karlsen T.H. (2007). “Variations in the MDR3 gene influences disease progression in PSC patients and disease suceptibility in epistatic interaction with a polymorphism in the OST-alpha gene.” Hepatology 46: 265A.

[18] : Oude Elferink R.P. and Paulusma C.C. (2007). “Function and pathophysiological importance of ABCB4 (MDR3 P-glycoprotein).” Pflugers Arch 453(5):601-10

[19] : Ziol M., Barbu V., Rosmorduc O., Frassati-Biaggi A., Barget N., Hermelin B., Scheffer G.L., Bennouna S., Trinchet J.C., Beaugrand M. and Canne-Carrie N. (2008). “ABCB4 heterozygous gene mutations associated with fibrosing cholestatic liver disease in adults.” Gastroenterology 135(1): 131-41

[20] : Wagner M., Zollner G., Trauner M. (2009). “New molecular insights into the mechanism of cholestasis.” J. Hepatol. 51(3): 565-80

[21] : Chapman R., Cullen S. (2008) ”Etiopathogenisis of primary sclerosing cholangitis” World J Gastroenterol. 14 (21): 3350-9

[22] : Smit J.J.M., Schinkel A.H., Oude Elferink R.P.J., Groen A.K., Wagenaar E., van Deemter L., Mol C.A.A.M., Ottenhoff R., van der Lugt N.M.T., van Roon M.A., van der Valk M.A., Offerhaus G.J.A., Berns A.J.M., Borst P. (1993): “Homozygous disruption of the murine mdr2 P-glycoprotein gene leads to a complete absence of phospholipid from bile and to liver disease.” Cell 75(3): 451-462

[23] : Mauad T.H., van Nieuwkerk C.M.J.,Dingemans K.P., Smit J.J.,Schinkel A.H., Notenboom G.E, van den Bergh Weerman M.A., Verkruisen R.P., Groen A.K., Oude Elferink R.P. et. al (1994) “Mice with Homozygous Disruption of the mdr2 P-Glycoprotein Gene. A Novel Animal Model for Studies of
Nonsuppurative Inflammatory Cholangitis and Hepatocarcinogenesis.” Am J Pathol. 145 (5) :1237-45

[24] : Fickert P., Fuchsbichler A., Wagner M., Zollner G., Kaser A., Tilg H., Krause R., Lammert F., Langner C., Zatloukal K., Marschall H.U., Denk H., Trauner M. (2004) „Regurgitation of bile acids from leaky bile ducts causes sclerosing cholangitis in Mdr2 (Abcb4) knockout mice." Gastroenterology 127:261–274.

[25] : Pikarsky E., Porat R.M., Stein I., Abramovitch R., Amit S., Kasem S., Gutkovich-Pyest E., Urieli-Shoval S., Galun E., Ben-Neriah Y. (2004) "NF-kB functions as a tumour promoter in inflammation-associated cancer" Nature 23;431(7007):405-6.

[26] : Katzenellenbogen M., Pappo O., Barash H., Klopstock N., Mizrahi L., Olam D., Jacob-Hirsch J., Amariglio N., Rechavi G., Mitchell L.A., Kohen R., Domany E., Galun E., Goldenberg D. (2006) "Multiple Adaptive Mechanisms to Chronic Liver Disease Revealed at Early Stages of Liver Carcinogenesis in the Mdr2-Knockout Mice" 15;66(8):4001-10.

[27] : van Nieuwerk C.M., Groen A.K., Ottenhoff R., van Wijland M., van den Bergh Weerman M.A., Tytgat G.N., Offerhaus J.J., Oude Elferink R.P. (1997) **"**The role of bile salt composition in liver pathology of mdr2 (-/-): differences between males and females.**"** J Hepatol. 26 (1): 138-45

[28] : van Nieuwkerk C.M., Elferink R.P., Groen A.K., Ottenhoff R., Tytgat G.N., Dingemans K.P., Van Den Bergh Weerman M.A., Offerhaus G.J. (1996) "Effects of Ursodeoxycholate and Cholate Feeding on Liver Disease in FVB Mice With a Disrupted mdr2 P-Glycoprotein Gene." Gastroenterology 111 (1): 165-71

[29] : Böcker W., Denk H., Heitz P.U., Moch H. (2008) "Pathologie" Urban & Fischer Verlag, München, Jena

[30] : Junqueira L.C., Bignolas G., Brentani R.R. (1979) "Picrosirius staining plus polarization microscopy, a specific method for collagen detection in tissue sections" Histochem J. 11(4):447-55

[31] : Lee H. S., Shun G.T., Chiou L.L., Chen C.H., Huang G.T., Sheu J. C. (2001) " Hydroxyproline content of needle biopsies as an objective measure of liver fibrosis: Emphasis on sampling variability" J Gastroenterol Hepatol. 20(7):1109-14

[32] : Löffler G., Petrides P., Heinrich P.C. (2006) "Biochemie und Pathobiochemie" Springer Verlag, Berlin, Germany

[33] : Vierling J.M. (2001) "Animal models for primary sclerosing cholangitis." Best Pract Res Clin Gastroenterol 15: 591–610.

[34] : Trauner M., Fickert P., Baghdasaryan A., Claudel T., Halilbasic E., Moustafa T., Wagner M., Zollner G. (2010) "New Insights into Autoimmune Cholangitis through Animal Models" Dig Dis 28(1): 99-104

[35] : Poynard T., Mathurin P., Lung Lai C., Guyader D., Poupon R., Tainturier M. H., Myers R. P., Muntenau M., Ratziu V., Manns M., Vogel A., Capron F., Chedid A., Bedossa P. (2003) "A comparison of fibrosis progression in chronicliver disease" J. Hepatol. 28: 257-265

[36] : Bissell D.M. (1999) "Sex and hepatic fibrosis" Hepatology 29:988–989

[37] : Ashcroft G.S., Dodsworth J., van Boxtel E., Tarnuzzer R.W., Horan M.A., Schultz G.S., Ferguson M.W (1997) "Estrogen accelerates cutaneous wound healing associated with an increase in TGF-beta1 levels" Nat Med;3:1209–1215

[38] : Lieber C.S.(1995) "Medical disorders of alcoholism" N Engl J Med 333:1058–1065.

[39] : Lammert F., Q.-H. Wang D., Hillebrandt S., Geier A., Fickert P., Trauner M., Matern S., Paigen B., Carey M. C. (2004) "Spontaneous Cholecysto- and Hepatolithiasis in Mdr2–/– Mice: A Model for Low Phospholipid–Associated Cholelithiasis" Hepatology 39(1): 117-128

[40] : Harnois D.M., Gores G.J., Ludwig J., Steers J.L., LaRusso N.F., Wiesner R.H. (1997) “Are patients with cirrhotic stage primary sclerosing cholangitis at risk for the development of hepatocellular cancer?” J Hepatol 27(3):512-6

[41] : Bergquist A., Glaumann H., Persson B., Broomé U. (1998) “Risk factors and clinical presentation of hepatobiliary carcinoma in patients with primary sclerosing cholangitis: a case-control study” Hepatology 27(2):311-6

[42] : Bergquist A., Ekbom A., Olsson R., Kornfeldt D., Lööf L., Danielsson A., Hultcrantz R., Lindgren S., Prytz H., Sandberg-Gertzén H., Almer S., Granath F., Broomé U. (2002) ”Hepatic and extrahepatic malignancies in primary sclerosing cholangitis ” J Hepatol 36(3):321-7

[43] : Malhi H., Gores G.J. (2008) “Cellular and Molecular Mechanisms of Liver Injury.” Gastroenterology 134 : 1641–1654

[44] : Safadi R, Friedman S.L. (2002) “Hepatic fibrosis—role of hepatic stellate cell activation.“ MedGenMed. 4(3): 27